AD-A139 815 WATER OPTICS OF THE MISSISSIPPI SOUNDS(U) NAVAL OCEAN RESEARCH AND DEVELOPMENT ACTIVITY NSTL STATION MS R A ARNONE DEC 83 NORDA-63 1/1

UNCLASSIFIED F/G 8/10 NL

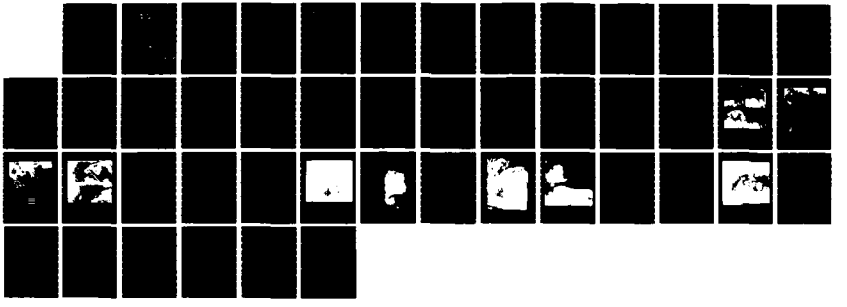

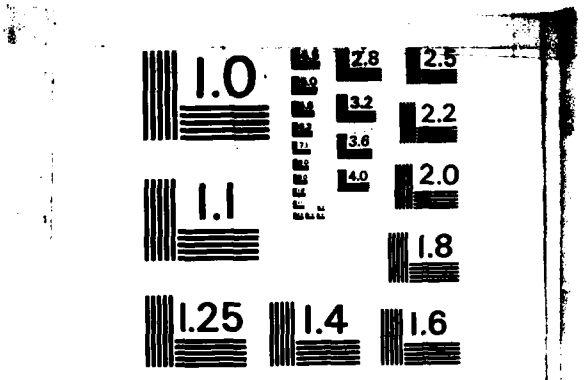

NORDA Report 63

Water Optics of the Mississippi Sound

Robert A. Arnone

Remote Sensing Branch
Oceanography Division
Ocean Science Directorate

December 1983

Naval Ocean Research and Development Activity
NSTL, Mississippi 39529

Foreword

An understanding of water optical properties in coastal waters is significant for mapping, charting, and geodesy applications since present electro-optical bathymetry mapping systems have limitations imposed by water turbidity. To study the spatial and temporal variability of coastal optics, remote sensing technology offers much potential. Through use of this technology, it is possible to develop improved environmental models of the physical and biochemical processes influence optical properties. Modeling the variability of coastal optics establishes operational planning for efficient deployment of electro-optical charting systems.

D. J. Phelps

G.T. Phelps, Captain, USN
Commanding Officer, NORDA

Executive Summary

From analyses of optical and suspended sediment properties in the Mississippi Sound, inherent relationships for exceptional turbid coastal waters are established. The optical parameters of secchi depth, Nepholometric Turbidity Units (NTU), and spectral upwelling and downwelling diffuse attenuation coefficients are correlated with themselves and with the size distribution of suspended sediments. From these relationships, estimates of other scattering and absorption water optical properties are established.

Coastal Zone Color Scanner (CZCS) and Landsat satellite data coincident with the experimental data were analyzed to access the spatial, temporal, and quantitative optical properties with the sound and surrounding shelf waters. Problems with atmospheric correction techniques in turbid coastal waters precluded obtaining quantitative optic measurements. Relationships between the spectral satellite radiance values and optical properties are established.

Acknowledgments

This work was sponsored by the Naval Air Systems Command Air 370G, program element 62759N, under program management by CAPT Ford. Appreciation is extended to members of Code 335, Naval Ocean Research and Development Activity, Remote Sensing Branch for their support with the field collection program and informal discussions. Mr. Dru Barrineau, of the Mobile District Army Corps of Engineers, was program manager for additional field work and data analyses used in this report. Dr. Peter Sherng of the Aeronautical Research Associates of Princeton, Inc., provided support in relating field data to numerical circulation models for the Mississippi Sound.

Contents

Illustrations

Illustrations (continued)

Tables

Water Optics of the Mississippi Sound

I. Introduction

An experiment was conducted in the Mississippi Sound in the northern Gulf of Mexico in September 1980. An evaluation of the spatial distribution of the optical properties was investigated by both ground truth data and satellite imagery analysis. The complex circulation of the sound can be somewhat characterized by the distribution of the optical properties. As in many coastal regions, the optical properties are influenced primarily by the high concentrations of suspended sediments. Since there appears a direct correlation between suspended sediment concentration and magnitude of local current patterns, a more thorough investigation of optical properties within highly turbid water was required in order to characterize spatial variability.

Water color can readily be sensed from satellite multispectral scanning systems (CZCS, Landsat). However, it is difficult to access absolute optical properties without making allowances for the atmosphere. Data from Landsat and the Coastal Zone Color Scanner (CZCS, Nimbus-7), was examined during this experiment and atmospheric correction techniques applied to quantify the optical properties.

The complex optical nature of coastal water has limited other investigators of optical properties of the two extremes: clear open ocean or turbid river waters. Investigations of the transitional coastal waters are limited. Techniques presently used for reduction of CZCS imagery for direction computation of concentrations of chlorophyll, suspended sediments, or the diffuse attenuation coefficient (Austin, Clark et al., 1980) have not specifically addressed high suspended sediment concentrations or coastal properties that are observed within the Mississippi Sound. This experiment addressed the inter-relationships of the optical properties within the Mississippi Sound and their determination from satellite systems. Problems associated with processing CZCS imagery for quantitative estimates of water parameters in coastal regions are also examined and errors are explained within the computations. Spacial variability of the water optical properties is discussed for both Landsat and CZCS imagery.

II. Study Area

Figure 1 illustrates the Mississippi Sound located in the northern Gulf of Mexico. A series of barrier islands is located approximately 7 miles to the south of the headland. This protected area extends from Mobile Bay on the east to Lake Ponchartrain on the west. The extremely low lying coastline in this area is composed of marsh and wetland areas. The waters are extremely turbid as a result of the high suspended sediments from various river outputs and the resuspension of silt-sized bottom sediments. The Mississippi Sound has a mean depth of 12 feet and bottom material is extremely soft silt. As a result, wind and tidal currents in this relatively confined basin resuspend bottom material quite frequently and the waters remain quite high in concentration of suspended sediment.

The character of the suspended sediments in the sound is highly variable as a result of the numerous river inputs. The rivers which include the Pearl in the west, and Jordon, Biloxi, Pascagoula, and Mobile in the east,

drain different basins and the size distribution, shape, and type of suspended sediments that are input into the sound are strongly variable. Once within the sound the tidal and wind mixing tend to horizontally and vertically distribute the suspended sediments. There are, however, gradual differences of suspended sediments that occur horizontally within the sound resulting from proximities of the river inputs. These spatial variations make it difficult to establish general relationships between optical properties and suspended sediment concentration for the entire sound, since the scattering and absorption of radiation is

Table 1. September 1980

Survey

Dates	9/2	9/8	9/9	9/10	9/20	9/21	9/24	9/25
Stations	4-40	6-40	44-68	68-80	2-42	44-80	4-36	38-66

Parameters Measured at Each Station

--Nephelometric Turbidity Units (NTU)
--Secchi depth
--Spectral (443, 520, 550, 670) Diffuse Attenuation Coefficient ("k")
--Total Suspended Sediments

Satellite Coverage

Date	Satellite	% Cloud Cover
9/9	CZCS*	30
9/14	CZCS/LS*	10
9/15	CZCS/LS	10
9/24	CZCS/LS	35

*Coastal Zone Color Scanner
*Landsat

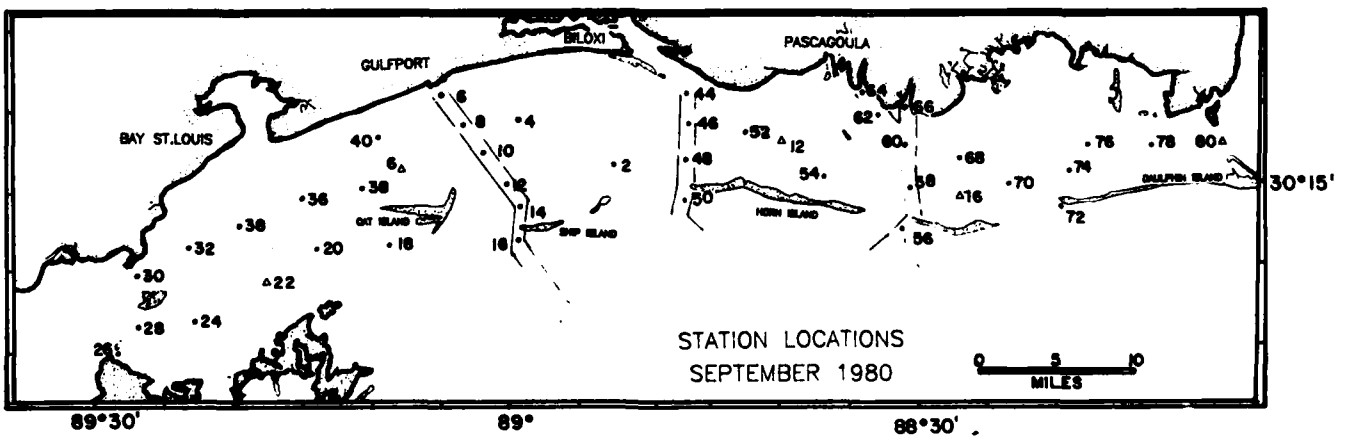

Figure 1. Mississippi Sound Experiment

dependent on the character of the suspended particles. Seaward of the barrier islands, on the southern boundary of the sound, the water clarity increases gradually. Turbidity plumes extending south from Mobile Bay and from channels between the islands can be observed on remote sensing imagery during the outgoing tides. A more thorough investigation of the tidal circulation was done by Sheng (1983) in which the general distribution of suspended sediments is well-correlated with the velocities of tidal currents.

Figure 1 also illustrates the 40 station locations occupied within the sound during September 1980. This experiment was a cooperative investigation with the Army Corps of Engineers. Their objective was to develop a circulation and suspended sediment model of the Mississippi Sound (Sheng, 1983; Sheng and Butler, 1982; Raytheon, 1981; and Isphording, 1981). Station locations were designed to collect water property data along major current flow areas, thus the entrance channels to Gulfport, Biloxi, and Pascagoula were well-sampled. A summary of stations occupied, parameters measured, and satellite coverage during this experiment is shown in Table 1.

III. Sample Procedure

A continuous flow-through system for measuring Nephelometric Turbidity Units (NTU) was installed onboard ship. Surface waters were pumped through the nephelometer and light scattering measurements were monitored. The instrument was calibrated daily, though little drift within the instrument was observed. This measurement was done with a wide band visible (Turner) photometer (Raytheon). The NTU measurement is a conventional technique for measuring water turbidity and is believed to be correlated best with suspended sediment concentrations, especially if the size distribution of the particles is known (Holyer, 1978). NTU measurements are not as sensitive to dissolved organic concentrations, i.e., hummic, fulvic, and tannic acids, since these constituents tend to mostly absorb the light field rather then scatter it. Since Mississippi Sound suspended sediment concentrations are significantly high, the scattering produced from these particles dominates the optical properties and the effects of dissolved organics is minimal.

A spectral irradiance meter with four interference filters centered at similar wavelengths as the Coastal Zone Color Scanner (443, 520, 550, 670 nanometers (nm) ±10 nm) was used to collect the downwelling diffuse attenuation coefficient "K_d". Although equipped with an upwelling irradiance sensor, the sensor was used on a limited basis to collect the upwelling diffuse attenuation coefficient, "K_u", since problems with instrument insensitivity were encountered. The irradiance sensors were equipped with cosine collectors and though not properly calibrated for absolute irradiance measurements, provided accurate relative measurements required for "K_d" and "K_u" determination. The instrument was lowered over the side of the ship and simultaneous underwater and surface deck irradiance measurements were collected at several depths within the water column.

Suspended sediments concentrations were determined at the surface and near the bottom at each station. A water sample was collected, and later filtered in the laboratory. The weight of the nonfilterable residue was then used to determine the suspended sediment concentration (Isphording, 1981). Several problems with the reliability of the values of the suspended sediment concentrations were experienced and reasons for possible error in sampling procedure will be discussed later. The size distributions of the suspended sediments for 15 surface water samples were made by weighing nonfilterable residue on 3 different size millipore

filters. Thus, the size distribution was catagorized into: > 8 microns (fine silt); 3-8 microns (very fine silt); and 0.4-3 microns (fine to coarse clay). It should be noted that the size distribution of suspended sediments greater than 8 microns was measured using a Coulter-counter. In all 15 samples measured, 99% of the samples had a size distribution less than 10 microns.

IV. Data Analyses

A. Transects

Specific transects through the Mississippi Sound have been illustrated for 9, 20, and 24 September 1980 (Fig. 2). These transects show general relationships of NTU, secchi depth, "K_d" values, and total suspended sediments, from coastal stations to seaward of the barrier islands. Note the station position by referring to Figure 1. The 9 September transect, along the Pascagoula channel, shows strong correlation between the optical values of NTU, secchi depths, and "K_d" values. At each of the station locations for this date, several samples of surface water were obtained and the range of concentrations of suspended sediments are displayed by the bars for each station. Because of the wide range of concentration, it is difficult to establish a strong relationship with the other water properties. Also, the values of the suspended sediments concentration are to be questioned.

Similar analyses of the surface water properties along the Gulfport channel transect, on 20 and 24 September, are also illustrated in Figure 2. The 20 September transect shows a strong correlation of the suspended sediment concentration and the optical water parameters. The downwelling spectral "K_d" measurements taken at 443, 520, 550, and 670 nm are shown to be strongly related to the other properties. Notice that the "K_d" 550 and "K_d" 520 values

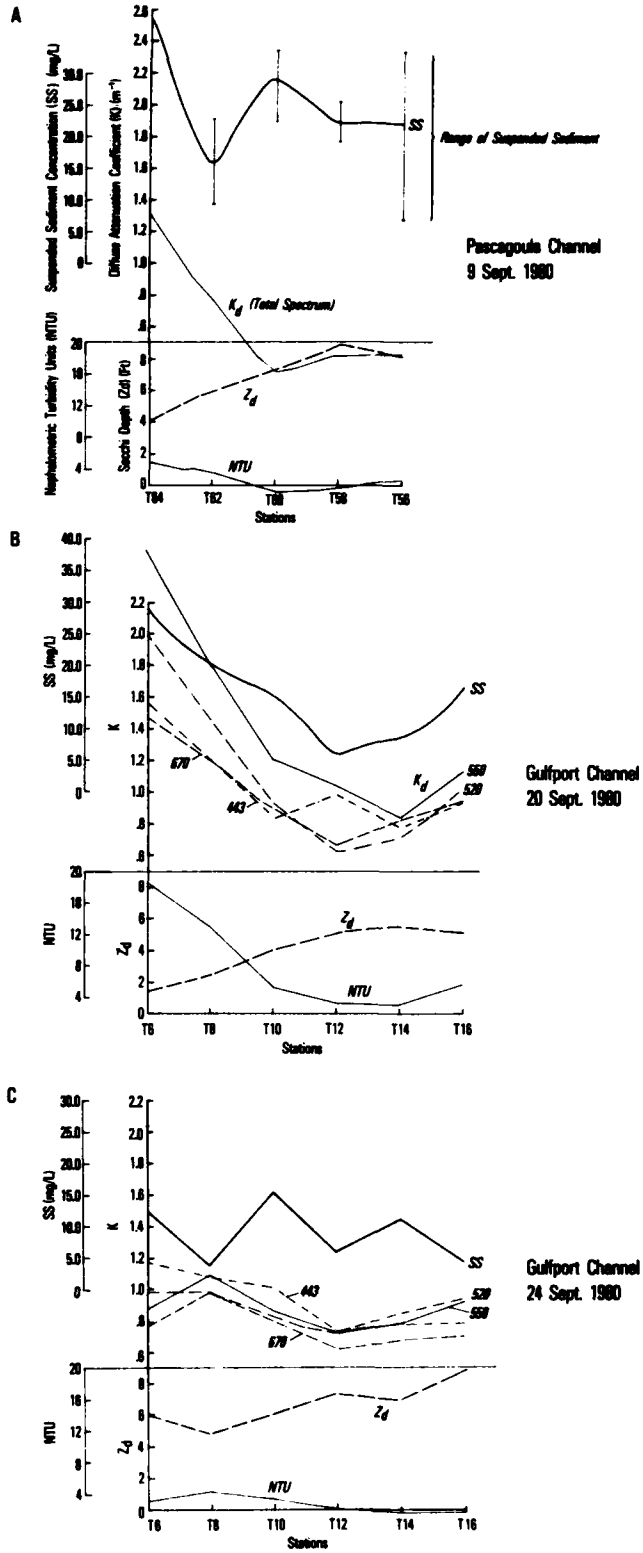

Figure 2. Distribution of optic properties and sediment concentrations along transects

have increased response as the water turbidity increases, i.e.; these "K" values have a greater dynamic range than the "K_d" 443, and "K_d" 670. This would be expected since the maximum light transmission for these waters occurs within these wavelengths. The temporal variability of the parameters can be shown by comparison of the 20 and 24 September transects. Data from each transect was collected within a 2-hour period: following high tide on 20 September and on an incoming tide on 20 September. The general increased clarity of the water shown in the transect for 24 September reflects the tidal inflow of offshore water all the way to the northern shore of the sound. The influence of the tidal forcing on the circulation within the sound has also been shown by the model developed by Sheng (1983).

B. Size Distribution of Suspended Sediments

In characterizing the optical properties of Mississippi Sound, the distribution of the size of suspended sediments within the sound should be examined since the optical properties are directly affected.

As was said previously, 99% of suspended sediments are less then 10 microns. From the analyses of the filtration of water samples, the suspended sediments range in size from a fine silt to a medium clay. This variation of size distribution is significant, especially in considering the optical scattering properties. Figure 3, taken from Holyer (1978), illustrates the relationships between NTU and sediment concentrations and the effects of particle size distribution. The figure indicates that for a NTU value of 25 the sediment concentration can range from 17 to 40 mg/l depending on whether the particle size is clay or silt. Also illustrated in this figure are the calibration standards taken from Stations 6 and 16 during the experiment. The data for these standards falls along the silt size particle line though some points indicate a smaller particle size.

Analyses of the particle size distribution of the suspended sediments are displayed in Table 2 and plotted in Figure 4.

As can be observed in Figure 4, the size distribution of the suspended samples are variable. The position of the data points is represented by the station number. There appears to be no noticeable correlation between station locations within Mississippi Sound and particle size distributions. One would expect a particle size distribution within the sound to reflect the locations of the various river inputs. However, tidal and wind forcing are significant in moving major water masses within the sound, which results in variable particle size distribution occurring throughout the sound. The result that the particle size distribution has on the optical properties can be characterized by comparison of Figures 3 and 4. Figure 4 illustrates the particle size ranging from a coarse clay,

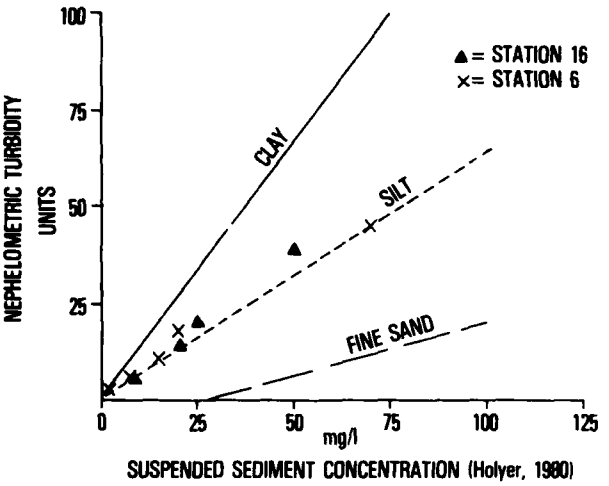

Figure 3. The relationship of NTU and Suspended Sediment Concentration is affected by size distribution. NTU calibration data points from the Mississippi Sound fall along the silt line.

<3μ (S12) to a fine silt, >8μ (S9). Using these extremes in Figure 3, for a sediment concentration of 25 mg/l, NTU values of 15-25 are possible. Similarly, for sediment concentrations of 75 mg/l, possible NTU values are 45-70. This demonstrates that with increasing sediment concentrations the effect of particle size becomes more pronounced on the NTU values. Similar effects on the diffuse attenuation coefficient would be expected.

C. Secchi Depth

A total of 136 secchi depth measurements were taken during the course of the experiment. This measurement, although extremely simple, provides a rapid, important method of determining water clarity. Gordon et al., (1978) suggest that this measurement, when combined with other optical measurements, can provide additional information about the water properties. The secchi depth measurement is strongly dependent on the backscattering probability that is directly related to the particle shape, size, and composition (not concentration). This is extremely important in relationship to remote sensing applications since the water cover results from an integrated backscattered radiation of the water column.

Figure 5 illustrates the relationship between secchi depths and suspended sediments for the Mississippi Sound. A regression of these variables resulted in a best approximation by a power equation, with a regression coefficient of 0.085. The large amount of scatter is quite disturbing at first glance and

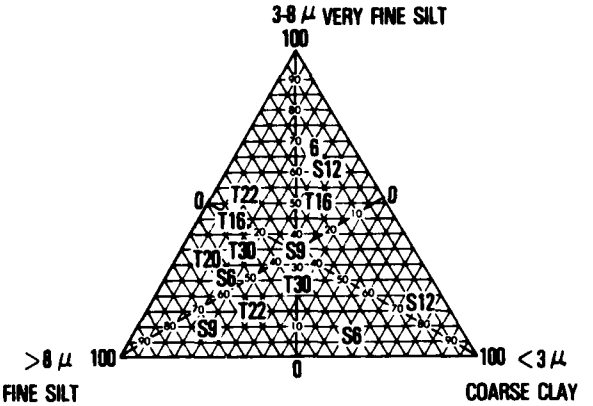

Figure 4. Size distribution of total suspended sediments for selected stations in the Mississippi Sound

Table 2. Surface suspended sediment size distribution by percentage

Station	Date	% > 8 microns (fine silt)	% 3-8 microns (fine silt-clay)	% < 3 microns (coarse clay)
S6	3 Sep	63.6	18.2	18.2
S6	25 Sep	36.6	9.6	60.8
S9	9 Sep	33.3	33.3	33.3
S9	25 Sep	72.5	72.5	5.0
S12	9 Sep	13.2	13.2	73.5
S12	24 Sep	15.4	62.0	23.1
T16	8 Sep	52.1	39.8	8.1
T16	24 Sep	23.9	50.0	26.1
T20	8 Sep	59.7	33.6	6.7
T20	20 Sep	62.7	27.7	9.6
T22	8 Sep	62.8	11.6	25.6
T22	24 Sep	45.5	0.0	54.5
T30	8 Sep	40.9	29.5	29.5
T30	24 Sep	55.1	8.2	36.7

the validity of the suspended sediment concentrations is in question. However, remember that the secchi depth measurement is not only dependent on concentration. The relationship between secchi depth and suspended sediments has been approximated by Manheim et al., (1970) and Gordon et al., (1978) to be

$$Z_d = w(k')/P \qquad (1)$$

where:

Z_d	=	secchi depth
k'	=	$\frac{ap}{bp}$
w	=	constant
ap	=	absorption of particles
bp	=	scattering coefficient of particles
P	=	particle concentration

This relationship has been shown to hold for waters of high suspended sediment concentration but low dissolved absorbers, i.e., yellow substance. The k' term is directly related to the size and shape distributions and not on the concentrations and is the coefficient by which the absorption and backscatter of particles are related. The importance of the k' term permits a better characterization of the interaction of the sediments properties and optical properties. The ratio of the backscattering of particles and water; (b_p/bw) is an index of the partical concentration (P). Figure 6 shows the relationship between bp/bw, i.e. (P), and Z_d at various k' and aw (the absorption coefficient of water plus dissolved materials). For waters that are free of dissolved absorbers; i.e. a_w=0, the curves in Figure 6 reduce to the hyperbolic relationship (Eq. 1). With waters that are high in dissolved absorbers, the Z_d-P relationship strongly depends on a_w for low P. Also note that at large P the position of the Z_d-P curve provides information on the value of k' while at low P information on a_w is obtained (Gordon et al., 1978).

Comparison of Figures 5 and 6 illustrates that for the Mississippi Sound

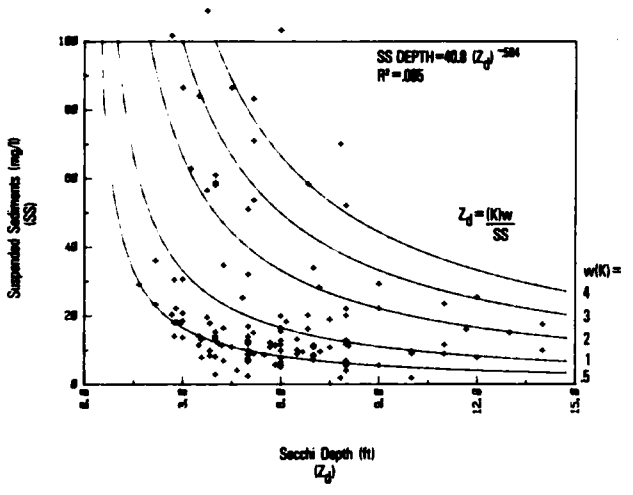

Figure 5. Relationship between secchi depth and the total suspended sediment concentration for the Mississippi Sound

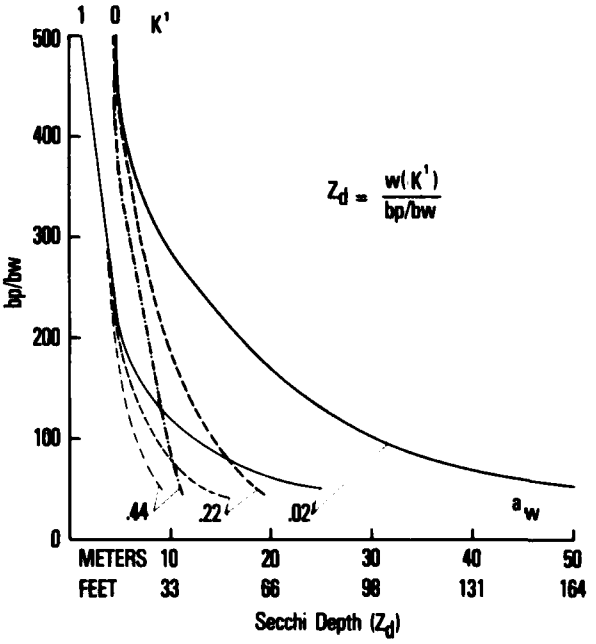

Figure 6. Z_d as a function of bp/bw, K^1, and a_w

waters, the effect of particle size, shape, and composition is significant in defining the Z_d-P curve. (Note that Fig. 6 is applicable out to Z_d of 50 m and that Fig. 5 extends only to 4.6 m.) For the shallow secchi depths the controlling parameter is the k' value and not a_w. Figure 5 has 5 curves superimposed over the data that result from Eq. (1) with various values of w(k') ranging from 0.5 to 4. The sound data tends to cluster along the curves 0.5 to 1 though some data also falls around the curve of w(k')=4. The position of the data points with respect to these curves provides a method of classifying the data into k' related properties that are based on shape, size, and composition of the particles. It should be noted that Mississippi Sound waters are not totally free of dissolved organic matter and that these absorption properties (a_w) of the water will effect this hyperbolic relationship. The relationships indicated in Figure 5 indicate that the size distribution of the suspended sediments appear to have a major influence in expressing any relationship between secchi depths and suspended sediment concentration. Additional work is required to more fully understand the size distribution on optical properties.

The relationship between secchi depth and NTU is illustrated in Figure 7. A strong correlation exists between these parameters. A power curve fit best approximates this relationship.

$$NTU = 75.98\ (Z_d)^{-1.748} \qquad (2)$$

The correlation coefficient has an R^2 value of 0.711. From examination, the distribution of the data appears to be a hyberbolic relationship between these parameters as described earlier, such that: NTU $\propto c/Z_d$. As was identified earlier, Z_d is strongly influenced by the backscattering probability, i.e. B = (0.05bw + bp Bp/bw + bp) where bw and bp are the scattering coefficients of water and particles respectively and Bp is the particle backscattering probability. NTU also are influenced by the scattering probability at 90°. Thus, by the strong correlation between NTU and Z_d, there also is a strong relationship between the scattering function at 90° and 180°.

The relationships between the spectral diffuse attenuation coefficient and Z_d are illustrated in Figures 8 and 9. The equation that best approximates this relationship is a power curve

$$K_d(\lambda) = AZ_d^{B} \qquad (3)$$

The coefficients, and regression correlation coefficients are listed in Table 3 for the various spectral wavelengths.

A strong correlation is noted between the $K_d(550)$ nm, and the secchi depth values. For the highly turbid waters of the Mississppi Sound, the maximum transmission of light for the preselected filters occurs closest to the 550 nm wavelength. The correlation for $K_d(670)$ is the poorest as a result of

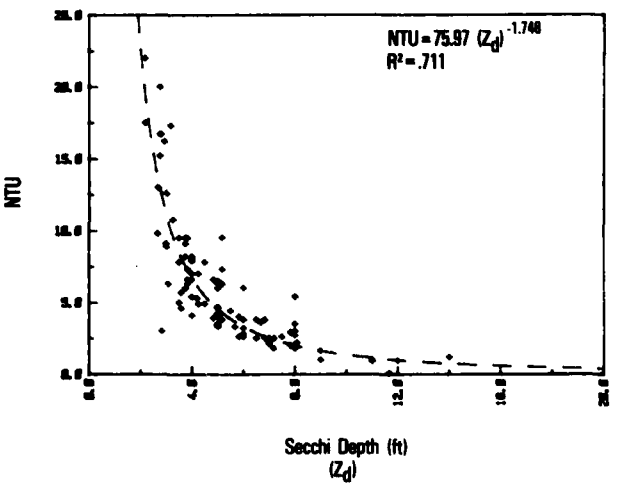

Figure 7. Secchi depth as a function of NTU

the strong water absorption in this part of the spectrum. Since the secchi depth measurement is responsive to the entire visible spectrum, the human eye selects that part of the spectrum of maximum penetrability to observe the disk. Thus it is reasonable for the $K_d(550)$ to best correlate with Z_d. It has been suggested that the Z_d and K are hyperbolically related (Holmes, 1970; Pool et al., 1929; and Gordon et al., 1978).

$$Z_d\bar{K} = n \qquad (4)$$

where $1.4 < n < 1.7$, (Fig. 10). Differences in "n" values result from both variation of size, shape, distribution of particles, and absorption of water in a similar way derived for Eq. 1. Comparison of Eq. 4 (Fig. 10) and the Mississppi Sound data results in Figures 8 and 9 confirming the hyperbolic relationship. A more thorough investigation of how the size distribution affects this relationship is required.

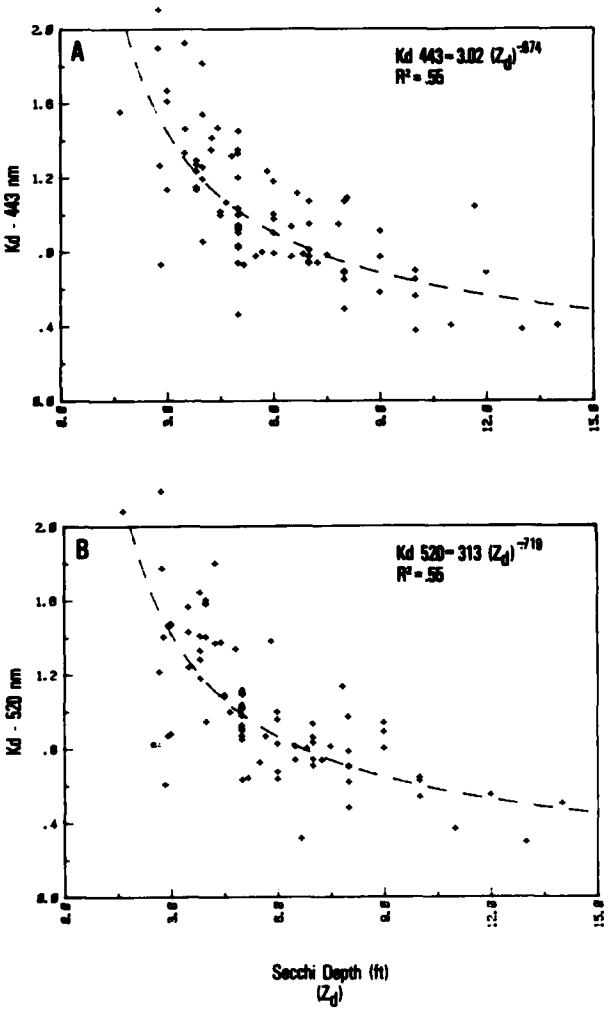

Figure 8. Secchi depth as a function of diffuse attenuation coefficient for 443 and 520 nm in the Mississippi Sound

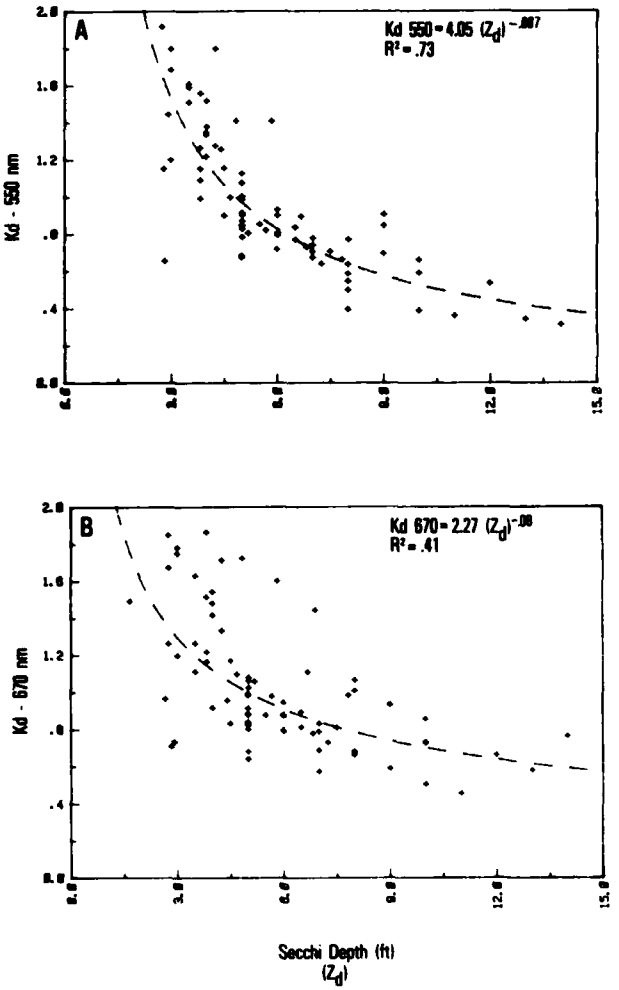

Figure 9. Secchi depth as a function of diffuse attenuation coefficient for 550 and 670 nm in the Mississippi Sound

The relationship between NTU and $K_d(550)$ and $K_d(520)$ is illustrated in Figure 11. The coefficients for the equations that best approximate a power curve are also shown in Table 3. A strong correlation exists between these parameters. The $K_d(550)$ correlates better with the NTU than the $K_d(520)$. The 520 nm wavelength previously was observed to correlate best with the secchi depth measurements (Fig. 9). As a result of the improved correlation of $K_d(550)$ with Z_d than with NTU, the forward scattering ($K_d(550)$) is better related to the 180° backscattering (Z_d) than with the 90° scattering (NTU). This confirms the assumption that the human eye selects the optimum wavelength (550 nm) in determining secchi depths.

Table 3. Coefficients for power curve for secchi depth and diffuse attenuation coefficient

$y = AX^B$

	A	B	R^2
$K_d(443)$ vs. Z_d	3.025	-0.674	0.551
$K_d(520)$ vs. Z_d	3.132	-0.719	0.553
$K_d(550)$ vs. Z_d	4.053	-0.887	0.728
$K_d(670)$ vs. Z_d	2.273	-0.512	0.417
$K_d(550)$ vs. NTU	0.476	-0.469	0.625
$K_u(520)$ vs. NTU	0.556	-0.372	0.461

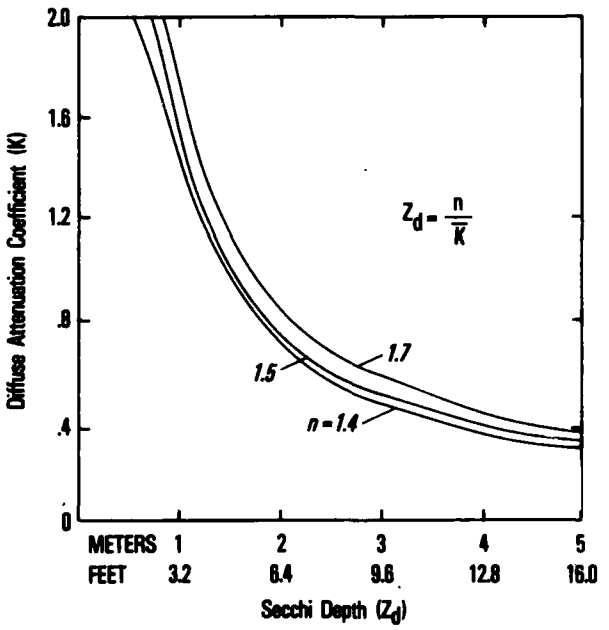

Figure 10. Secchi Depth as a function of diffuse attenuation coefficient for various "n"

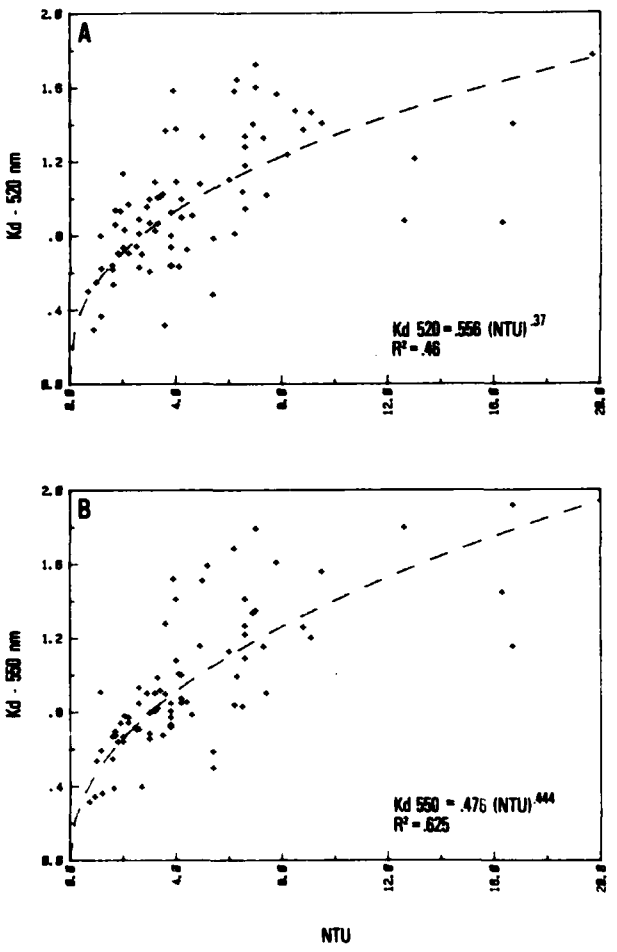

Figure 11. NTU as a function of K_d for 550 and 520 nm for the Mississippi Sound

D. K_u Versus K_d

For a small number of stations, the upwelling (K_u) as well as the downwelling (K_d) diffuse attenuation coefficients were measured. For remote sensing applications, the direct calculation of K_u has been suggested to be more relevant since it is more closely associated with what the remote sensor senses (Austin, 1978). However, because of the high suspended sediment concentration within the sound, the flux of upwelling irradiance was beyond the resolution of the instrument used in this measurement and only at several selected stations were reliable measurements obtained.

The relationship between upwelling (K_u) and downwelling (K_d) diffuse attenuation coefficient is illustrated in Figure 12 for the 443, 550, and 670 nm spectral channels. If we assume a linear relationship between K_u and K_d, Table 4 indicates the correlation coefficients and the regression coefficients for these spectral K values.

From examination of Table 4, notice the relationship for the 550 nm spectral band has the lowest regression coefficient between upwelling and downwelling "K" as compared to the two other spectral bands, 443 and 670.

Notice in Figure 12 that in the 550 nm channel the $K_d(550)$ is greater than the corresponding $K_u(550)$ value. (The slope of the linear relationship is <1.) The rate of attenuation is greater for light propagating into the water than for light propagating out of the water. Since the 550 nm wavelength has relatively high transmission in these particular waters, light is being scattered and propagated upward from deeper water depths than for the other wavelengths which have a shallower penetration depth. This increased amount of upwelling light is attentuated at a lower rate than the downwelling light for this wavelength, (550 nm). The y-intercept (A) for the 550 nm relationship has a value very close to 0, (-0.06).

The dependence of the solar altitude attributes to the variation in K_u and K_d. Since the majority of the visible light entering the water column in the 550 nm wavelength comes from the sun, as opposed to skylight, the rate of attenuation of this downwelling radiation depends on the altitude of the sun. This is especially true for turbid waters where there is much scattering and attenuation in the upper layers. For upwelling radiation, the radiation field is more diffuse since it results from the multiple scatters of the downwelling flux. The downwelling attenuation rate will be greater than the upwelling attenuation rate as a result of this "point" radiation source (sun). This difference in rate of attenuation is illustrated in Figure 12 for the 550 nm wavelength. Note also that the near zero intercept (0.06) indicates that for clear waters the dependence on the solar altitude has a diminished effect and a similar attenuation rate for upwelling and downwelling radiation is observed. With increasing water turbidity the difference in K_u and K_d become more significant. This increased difference for turbid (coastal) waters will be discussed later when compared to satellite (CZCS) applications.

Table 4. Correlation between upwelling and downwelling diffuse attenuation coefficient, $K_{u(\lambda)} = A + B(K_{d}{}^{\lambda})$

	A	B	R^2
K(443)	-0.013	0.845	0.698
K(550)	-0.062	0.710	0.522
K(670)	-0.238	0.929	0.637

Plot "A" of Figure 12 illustrates the K_u and K_d at 443 nm. At this shorter wavelength, increased atmospheric scattering increases the intensity of skylight, thereby decreasing the influence of the solar altitude. The downwelling radiation has a more diffuse character, similar to the upwelling light field. This relates in increased similarities between the rates of attenuation in K_u and K_d. The slope of this relationship is approaching 1 (0.84). Again notice that in clear waters $K_u = K_d$, while in more turbid waters the downwelling attenuation rate is greater.

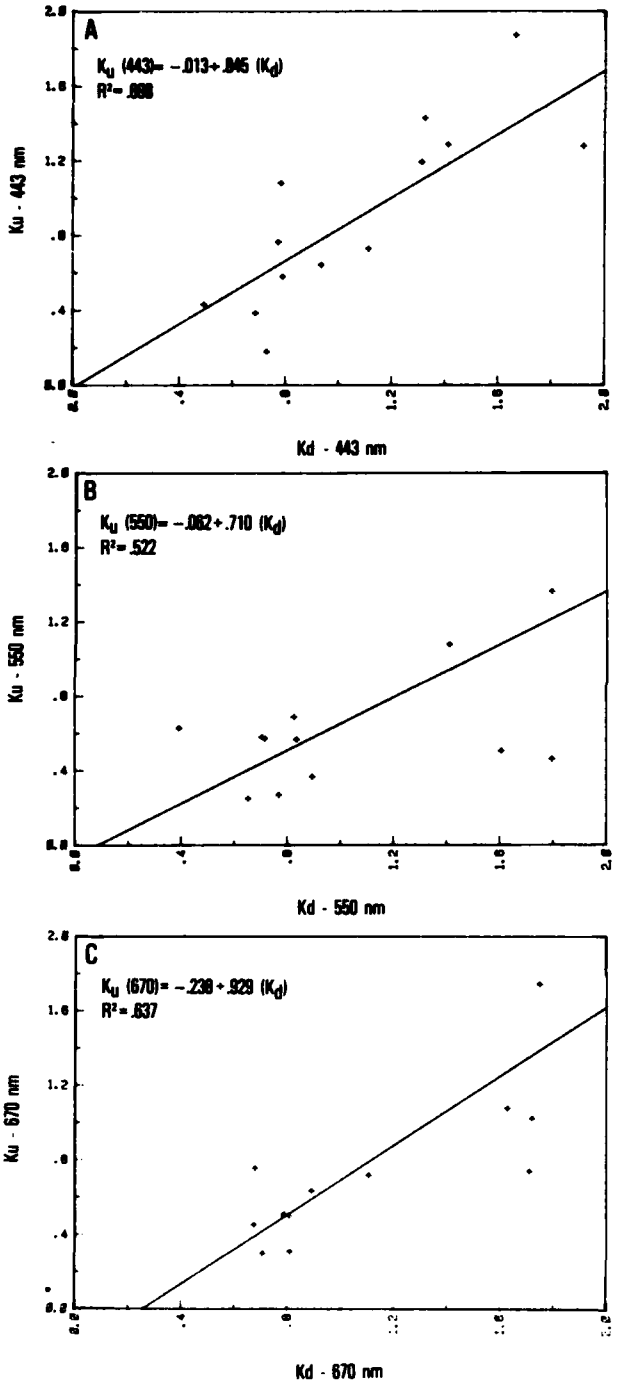

Figure 12. K_d as a function of K_u at 443, 550, and 670 nm

The relationships of K_u and K_d for the 670 nm channel are illustrated in Figure 12. Because at this wavelength, light is attenuated rapidly in the upper meters, a minimal amount of scattering and upwelling radiation is expected. From this figure (Plot C) the significance of the non-zero y-intercept is not fully understood. One could speculate that for clear waters the downwelling attenuation rate results only from absorption and that because little scattering occurs, there is minimal upwelling radiation. Thus, there cannot be an upwelling attenuation rate. Therefore, a $K_d(670)$ value of 0.2 has a value of 0 for $K_u(670)$. Further investigations are required to more fully understand what occurs in the longer wavelengths.

V. Satellite Imagery

As a result of the high percentage of cloud cover in Mississippi Sound during the September experiment a limited number of satellite imagery was analyzed.

A major objective of this experiment was to relate the measured optical properties to the radiance values of the satellite data. From results published by Austin (1980), the ratio of the upwelling radiation of two CZCS channels is directly related to the diffuse attenuation coefficient. For Landsat imagery, it is difficult to determine absolute radiation values and thereby difficult to obtain optical properties directly.

The application of CZCS and Landsat MSS for obtaining the spacial variability of water optical properties has been discussed by various investigators, (Aranvachapun, et al., 1981; Austin, 1980; Munday, et al., 1979; Clark, et al., 1980; and Sturm, et al., 1980). An evaluation of these sensors in determining water properties has not been adequately demonstrated because of the dissimilarities of each sensor system. That is to say, each sensor has specific characteristics for measuring ocean/coastal environments; therefore, an evaluation should be based on the application of the data.

The CZCS sensor has an 800 m spatial resolution and has a repeat time of approximately 1.3 days. CZCS channels are ±10 nm, centered at 443, 520, 550, 670, and 750 nm (Hovis, et al., 1980). The channels have been selected for water property applications and are sensitive to deep ocean property variations where the color variability is relatively small. Extensive calibration has been inherent to CZCS to provide absolute radiometric values of the light field. The Landsat system, having 80 m spacial resolution with a repeat time of 18 days, was mainly designed for land applications. The channels are, therefore, wide, ±50 nm, and are centered at 550, 650, 750, and the last channel is from 800 to 1100 nm. The application of Landsat for ocean/coastal applications has been confined mostly to the coastal/shelf water areas. This is because of the high spacial resolution of the sensor and its corresponding reduced coverage, and the inability to sense subtle color variations. Special resolution is required in coastal areas where the variability of water properties is changing dramatically. In many coastal areas, "water color" changes occur such that Landsat sensors have sufficient dynamic range to distinguish the spacial variability. The subtle color changes observed in the deeper ocean waters have more limited applications to Landsat. In addition, the repeat time greatly hampers the utility for evaluating the variability of the coastal processes that occur on a time scales between 12 hours (tides) to several days.

Algorithms of equating absolute satellite radiometric values to optical and chemical parameters have been developed mostly for CZCS and on a limited basis for Landsat (Aranuvachapun, et al., 1981; Austin, et al., 1980; Clark, et al., 1980). These algorithms require absolute upwelling radiation measurements from the water column and this requires accurate atmospheric correction. This correction is a serious source of error for determining water properties. On examination, this approach with CZCS data has definite drawbacks in coastal areas and is more limited for Landsat data since the sensitivity to upwelling radiation is reduced and this results in making Landsat data more sensitive to atmospheric correction.

A. Influence of Water Types on Water Optical Properties

The application of remotely sensed data for determining the distribution of water optical properties is more strongly associated with radiation sensed by the satellite than biochemical parameters such as chlorophyll or suspended sediments. The scattering and absorption of light within the water column gives rise to the water color or the upwelled radiation. Optical properties are direct functions of scattering and absorption and are more closely associated with upwelling radiation than the bio-chemical parameters. It follows that optics should correlate better with the remotely sensed data.

Optical properties of waters are affected by different concentrations of suspended sediment, chlorophyll, dissolved organic material, and by the size and shape of the suspended particles. In coastal areas, where there are great variabilities of these parameters, complex relationships between

water optics and the parameters can be applied. Certain parameters have a dominating influence on optical properties for different water types. (A dominant influence is regarded in context to upwelling or remotely sensed radiation.) In coastal waters, the dominant parameters are suspended sediment concentrations; whereas, in the deeper ocean water, sediments are minimal and chlorophyll concentration is more significant. As concentrations increase for each of these water masses, the other parameters have less influence on optical properties. What occurs in the transitional (shelf) waters is some combination of these parameters and is presently an area of research. Generally, it is said that the parameters influence optics in coastal and deep oceanic waters are different and will have different response in multichannel remotely sensed data. It becomes difficult to distinguish the various influential constituents within the water column, even though applying the spectral relationships. This results from the interaction between parameters that have second order effects on the optical properties. However, because optical properties result from this interaction and results in the upwelled radiation field, the properties should be closely related to the remotely sensed radiation.

B. Atmospheric Correction Techniques and Problems

Previous investigators have used Landsat data to correlate directly between ground truth and radiometric values from the satellite. The development of algorithms then was derived from a regression relationship. Because of the various differences from scene to scene, it was impossible to use the same regression algorithm. The requirement for universal algorithms to eliminate the necessity of ground truth measurements has led to obtaining absolute upwelled radiation from the ocean from satellites.

The absolute measurement of the upwelled light field from the ocean has been related to the diffuse attenuation coefficient, (Austin, et al., 1980), chlorophyll (Gordon, et al., 1980), and suspended sediments (Clark, et al., 1980). These algorithms were derived from absolute upwelling radiation from ground truth and are assumed to be universal. However, the problem remains of obtaining absolute upwelling radiation from the water column from the satellite.

Absolute measurements of radiation from satellite require non-drifting optics or a calibrated source within the spacecraft. Landsat has had significant problems in this area, although some progress has been made (Ahern, et al., 1978). CZCS calibration has been better; however, problems with outgasing within the satellite have defined an exponential decay of the original calibration coefficients, based on its orbit number (Goddard Space Flight Center, personal communication).

Another serious problem arises from defining the effects that the atmospheric aerosols have on the satellite sensed radiation. An atmospheric correction technique proposed by Gordon (1978); and Gordon, et al., (1980) applies spectral channels in a weighted subtraction of red (670 nm) or near infrared channel (750 nm). This technique is presently applied to CZCS although a similar approach can be applied to Landsat (Aranvachapan, et al., 1981).

The correction algorithm takes the form:

$$t_\lambda L_{U\lambda} = L_{T\lambda} - L_{R\lambda} - \left(\frac{\lambda o}{\lambda}\right)^\eta \frac{F\lambda}{F_\lambda o}\left[L_{T\lambda o} - L_{R_\lambda o}\right] \qquad (5)$$

where

L_u = upwelled radiance at sea surface

λ = wavelength of interest

L_T = total radiance at satellite

λ_o = reference wavelength

L_R = rayleigh radiance

F_λ = solar flux

η = angstrom coefficient

t_λ = air-sea transition

In generating this equation the upwelling radiation from the water column at the reference wavelength is assumed zero or that the radiation sensed in this channel is atmospheric; i.e., Rayleigh and aerosol scattering only. Presently, the 670 nm channel is used as the reference in CZCS imagery. In coastal areas where there is high sediment concentrations upwelling radiation occurs at 670 nm. For these type waters, the correction subtracts water color in addition to the atmospheric aerosols. In deeper oceanic waters, where the optical properties are dominated by the chlorophyll concentration, the assumption of zero upwelling radiation at 670 nm is more valid. Transitional waters are still under investigation to determine the amount of upwelling radiation that occurs at 670 nm.

The angstrom coefficient, η, is another variable within the correction that presents difficulty. Clear water radiance methods have been suggested by Gordon, et al., (1981) to determine η. Through selection of areas within the image in which clear water is assumed, the radiation sensed by the satellite can be related to the optical aerosol thickness of the atmosphere. Following this, the resulting angstrom coefficient can be computed.

This application is difficult for coastal areas where there is little "clear water." The technique usually requires a selection of an area farther offshore and the result is applied to the coastal area. A common problem is that the aerosol optical thickness (η) can change over coastal and deep ocean waters. For these cases, the resultant absolute radiance calculation can be significantly in error.

Atmospheric correction directly influences the determination of optical parameters from satellite data since the universal algorithm requires absolute measurements of upwelling radiation from the water column. Since the upwelling radiation from the sea surface is approximately 5-10% of the total radiation received by the satellite sensor, accurate atmospheric corrections are critical for accurate measurements of water optics.

C. Satellite Data Analyses

Numerous CZCS and Landsat imagery were analyzed over the Mississippi Sound area during September 1980. Unfortunately the weather conditions were not optimum for collection of satellite imagery. The summer months along the northern Gulf coast have extremely humid, thick atmospheres.

Landsat imagery is collected at approximately 9:30 a.m., local time, and CZCS is taken approximately 2 hours later at 11:30 p.m., local time. During several instances, near-coincident (2 hours) CZCS and Landsat imagery of the study area was collected and analyzed. As appears to be typical in experimental design, the clearest two days for satellite imagery were not incident with ground truth. However, an evaluation of each sensor's ability to detect coastal color changes of the study area can be demonstrated.

Processing of satellite data was done on the Interactive Digital Satellite Imaging Processing Systems (IDSIPS) located at the Remote Sensing Branch of NORDA. The imagery used for this report

are in color; however, the black and white imagery used in this report is somewhat limited in coastal feature recognition.

Figure 13 is a mosaic of CZCS imagery of the 9 September 1980, in which 4 spectral channels are illustrated. The amount of cloud cover in this image significantly hampers the recognition of oceanic features. The atmospheric correction was applied to this imagery to obtain absolute upwelling radiation from the water column. The 670 nm channel was used as the reference channel. Upon examination of Figure 13, note that the Mississippi Sound and entire Gulf coast area is saturated and appears white in the 670 nm channel. Weighted subtraction of this channel from the others would be essentially subtraction of a constant and could result in negative or very small upwelling radiances from the coastal waters. Since the algorithms for computing the diffuse attenuation coefficient require positive upwelling radiation, a closer examination of the atmospheric correction is required. The resultant atmospherically corrected image for the 443 channel is illustrated in Figure 14. This full resolution CZCS image is displayed as 512x512 pixel and has been registered to a Mercator projection. Notice that the coastal waters in the Mississippi Sound appear black since the corrected upwelling water radiation is less than a value of zero. In the southern portion of the image, the deep oceanogrphic features are more clearly visible by the tongue-shaped position of the Loop Current. For this image the clear water radiances were selected in the Loop Current and the angstrom coefficient (n=Ø) determined for the entire image. The Loop Current waters are considered good, clear water because of previous ground truthing; yet when the computed angstrom coefficient was applied to the coastal area, negative radiance values resulted. In images of other coastal areas where there is not "clear water" the selection of the angstrom coefficient becomes extremely difficult.

For the 9 September 1980 image, there are several possible explanations for the negative upwelling radiance for the 443 nm channel in the coastal waters. There is significant upwelling of radiation from the water in the 670 nm channel, such that the subtraction of this channel drives the other channels negative. This is very possible in coastal areas where the high chlorophyll results in very small upwelling radiance at 443. Another problem is associated with varying angstrom coefficients between coastal and deep water areas. To evaluate this, an image was generated for n=Ø and n=Ø 2 (Fig. 14 and Fig. 15). (The imagery illustrated in these figures was displayed such that negative numbers are represented as tonal gradations to positive numbers.) In both images, the absolute radiance values of the upwelled radiation in the coastal region are still negative. The coastal features in Figure 15 (n=2) are more recognizable than in Figure 14 (n=Ø). For the offshore waters in the vicinity of the Loop Current, the water mass features are better observed by Figure 14 (n=Ø). This illustrates that a variable spacial angstrom coefficient or optical aerosol thickness is occuring within this image. As would be expected, higher aerosols closer to the continent have a higher aerosol optical thickness.

In Figure 16, full resolution CZCS is illustrated in the top portion and the Mississippi Sound area is magnified by 2 in the lower portion. The imagery has been corrected atmospherically and Mercator registered. The coastline has been overlayed for clarity. Coastal water features are clearly observed and positive upwelling radiance values were computed. The distribution of the lighter tones correspond to various color changes resulting from various sediment concentrations. Similar results as shown in this figure were obtained for the 550 nm channel of CZCS.

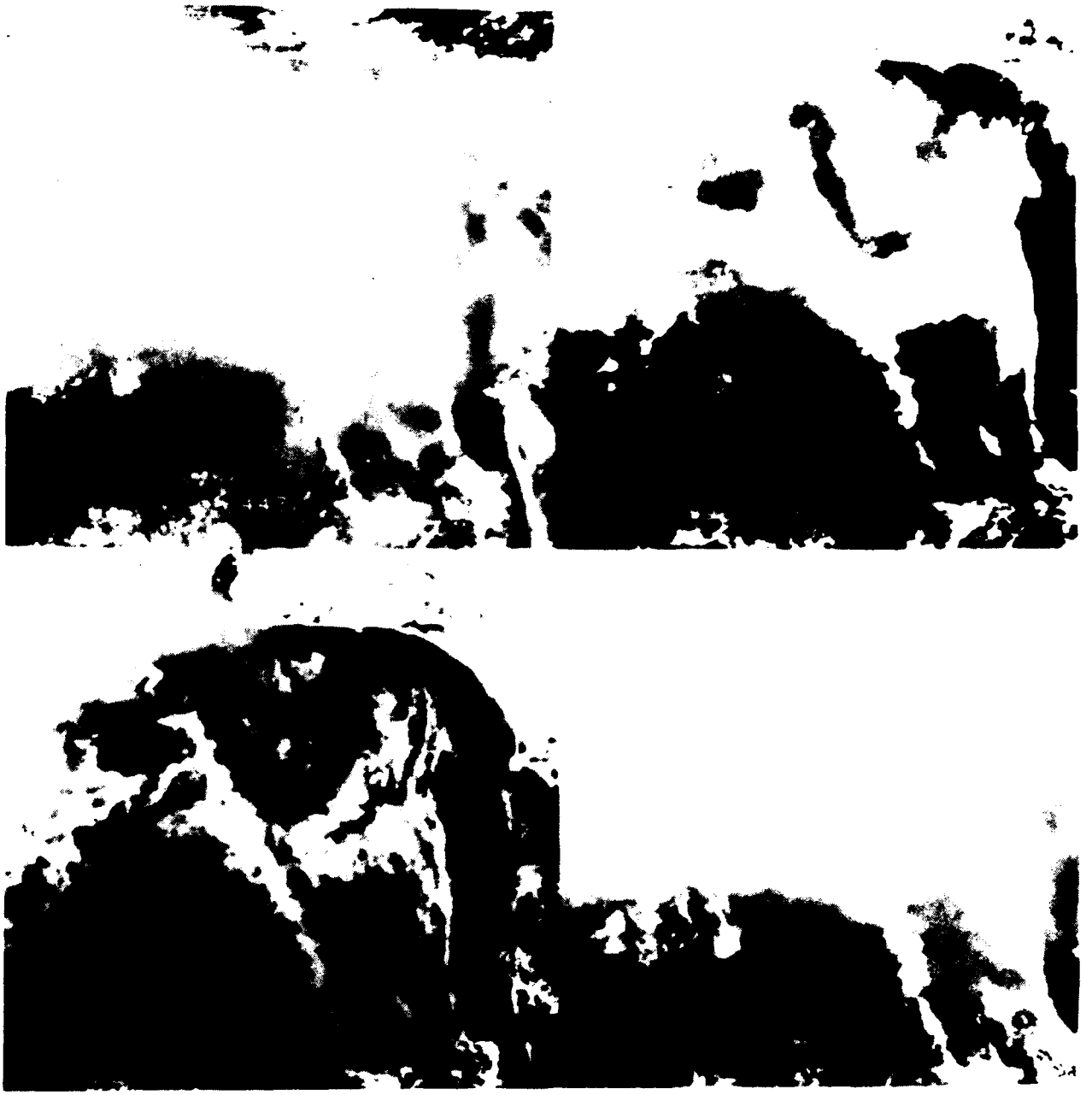

Figure 13. CZCS uncorrected imagery, 9 September 1980, spectral channels 443, 520, 550, and 670 nm

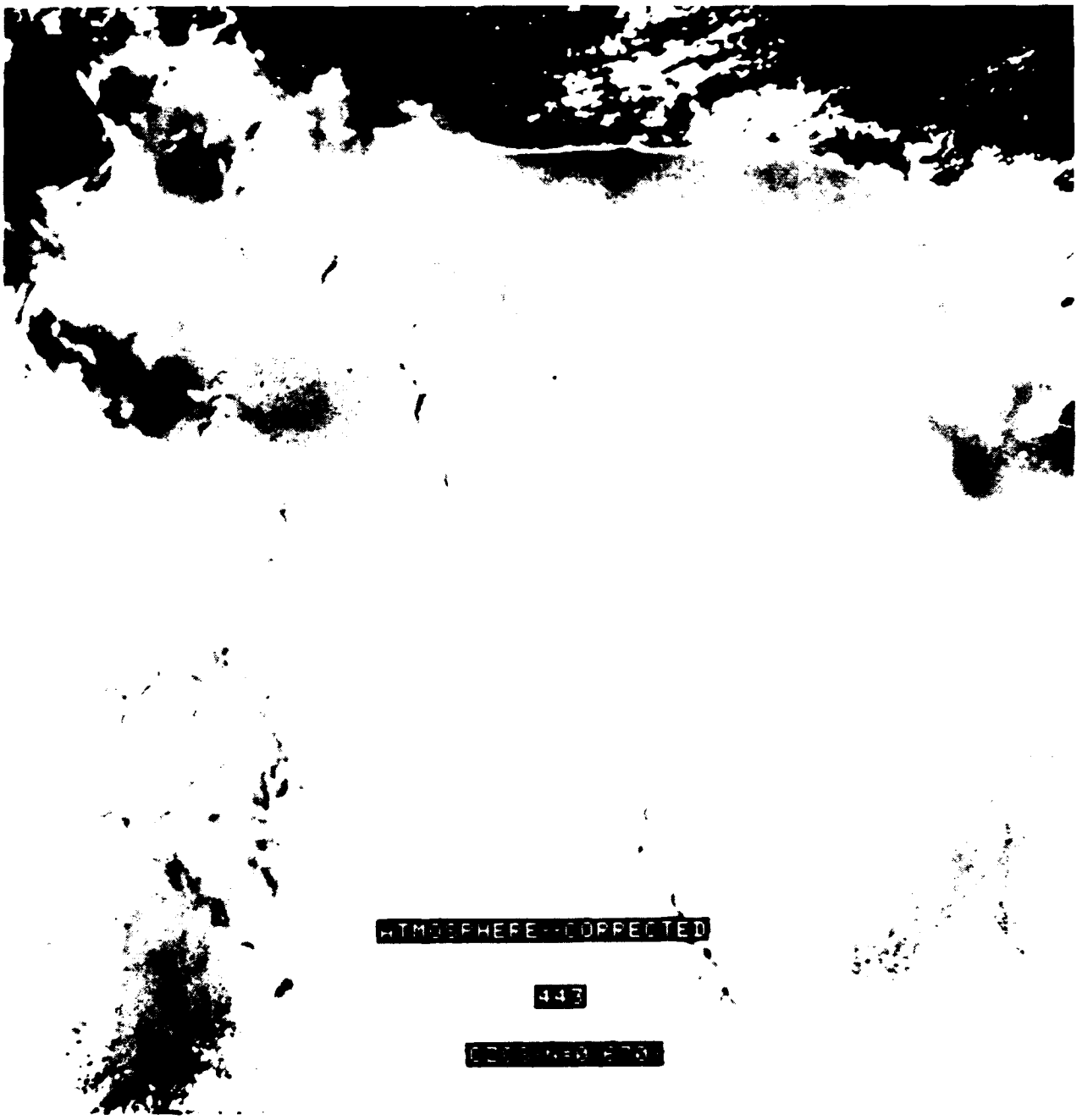

Figure 14. CZCS imagery atmospherically corrected, 9 September 1980, channel 443 nm (angstrom coefficient = 0)

Figure 15. CZCS imagery atmospherically corrected, 9 September 1980, channel 443 nm (angstrom coefficient = 2)

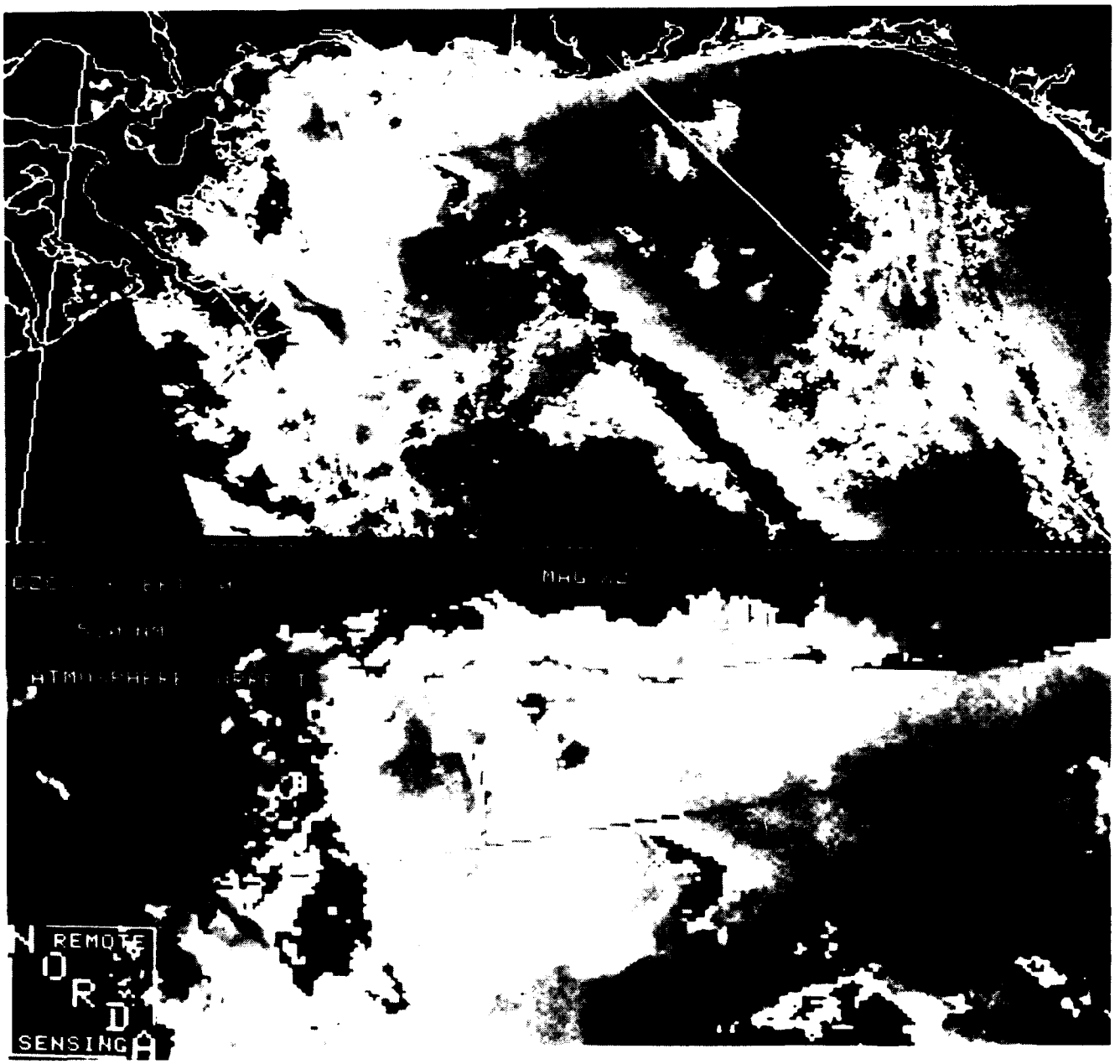

Figure 16. CZCS imagery atmospherically corrected, 9 September 1980, channel 520 nm

However, the "K" algorithm (Austin, 1980) requires a positive ratio using the 443 nm channel and since this was negative, "K" cannot be determined in the coastal waters.

The suspended sediment algorithm (Clark, et al., 1980) that used the ratio of 520 to 550 nm was applied to this image and major discrepancies with ground truth were observed. This indicates that computations of upwelling radiation in these channels, although positive, are in error also as a result of the atmospheric correction process.

As a result of the problems with the atmospheric correction in coastal waters, an investigation of the correlations between the raw CZCS count values (0-255) and the optical properties is illustrated in Figures 17, 18, and 19. These figures illustrate ground truth data for the diffuse attenuation coefficient (K), NTU, and suspended sediment concentration for 443, 520, and 550 nm channels on CZCS.

The data used for this analysis in Figures 17, 18, 19 came from stations t44 t66 plus S9 and S12 (Fig. 1). These stations are located in the central eastern portion of the sound yet display variations in water types at this location. A grouping of the suspended sediment concentration of the eastern Biloxi channel data and Pascagoula channel data is shown in this figure as representative of the eastern and western data points. A similar clustering is not reflected in the NTU or K values. As previously indicated, the optical properties are not only related to sediment concentrations but also dependent on the shape, size and composition of the suspended material.

The application of the 550 nm channel is highly limited for these ground truth correlations since the channel is saturated at 255 (Fig. 19). The chlorophyll absorption channel (443) (Fig. 17) has lower count values than the 520 nm channel (Fig. 18). As a result of the high suspended sediment and chlorophyll concentrations it is difficult to determine exactly what the 443 is responding. The 520 nm channel (Fig. 18) illustrates the best correlation with the ground truth.

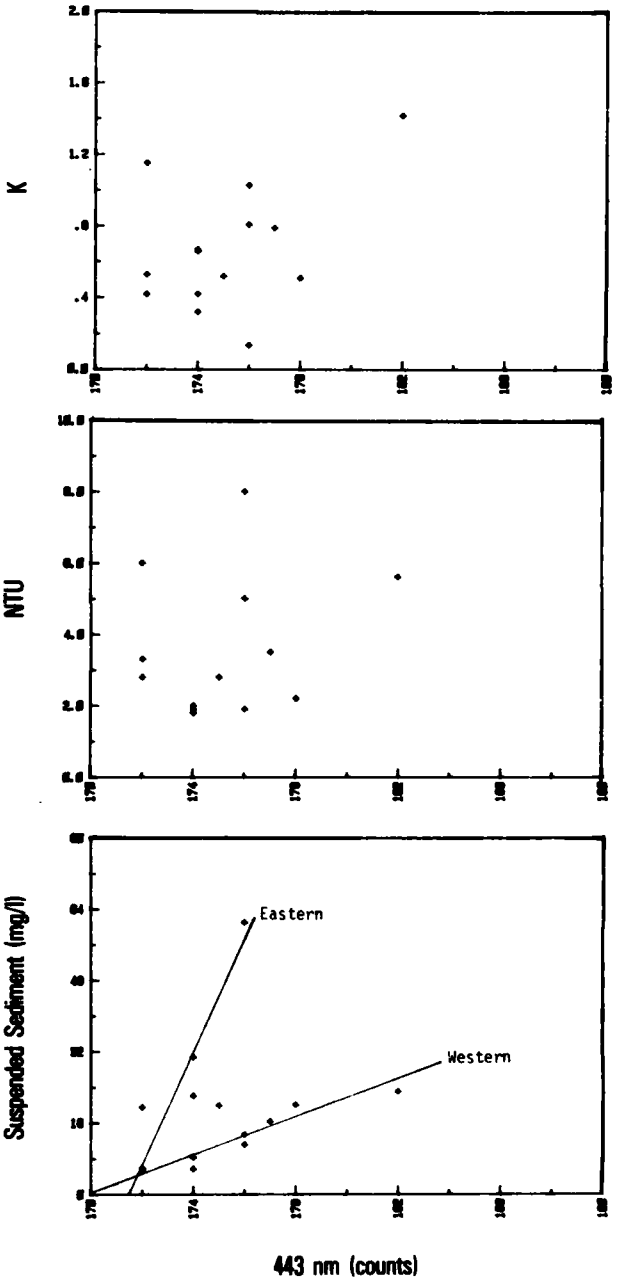

Figure 17. Relationship of CZCS count values, 9 September 1980, and ground truth (443 nm)

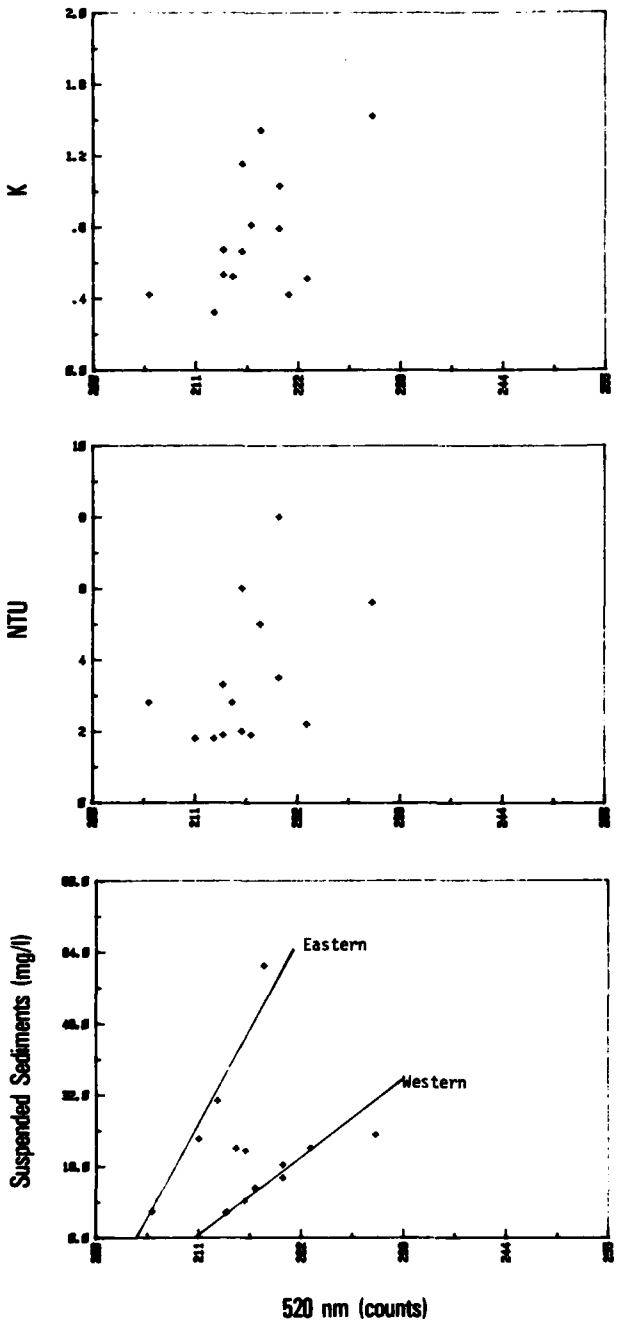

Figure 18. Relationship of CZCS count values, 9 September 1980, and ground truth (520 nm)

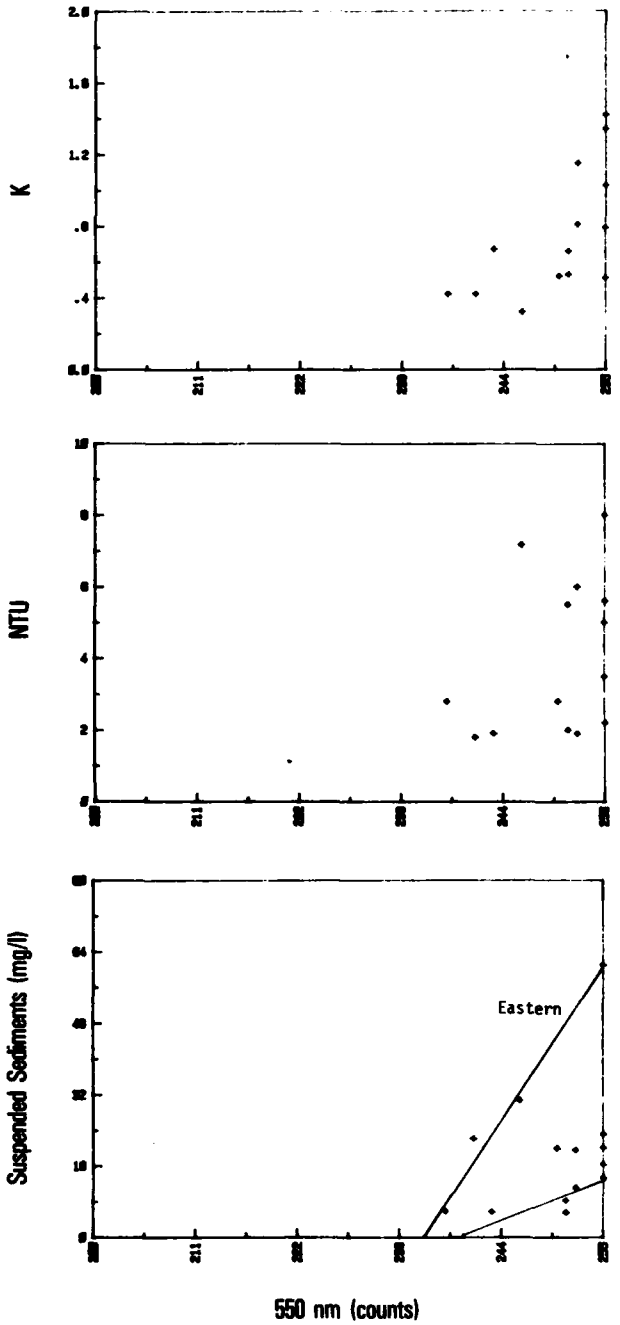

Figure 19. Relationship of CZCS count values, 9 September 1980, and ground truth (550 nm)

1. 14 September 1980

The 14 September 1980 analyses of CZCS data is illustrated in Figure 20. The CZCS image was atmospherically corrected in a similar method previously described and represents upwelling radiation in the 520 and 443 nm channels. Similar problems of negative values of upwelling radiation in coastal waters were experienced. The image has been registered to a Mercator projection and the coastline superimposed for clarity. The image is displayed with a negative minimum threshold. In other words the image has been enhanced to extract the ocean/coastal features though the values are not absolute and cannot be applied to universal algorithms.

Notice in Figure 20 that the 520 nm channel shows significantly bright tones in the eastern portion of the Mississippi Sound. These are most likely a result of high suspended sediments. In the eastern portion of the sound the tones are darker, especially along the coast. Along the offshore barrier islands brighter tones are observed. In the 443 nm channel, the entire sound has a characteristic dark tone indicating a high chlorophyll content. The eastern sound, which has high suspended sediment concentrations, has somewhat lower 443 count values than the rest of the sound as a result of the lower chlorophyll concentration from reduced light penetration in turbid waters. The western portion of the sound indicates high chlorophyll absorption by the very dark tones in the 443 nm channel. For these coastal waters, the interaction between water turbidity and chlorophyll concentration is an important mechanism in understanding the various imagery in various CZCS channels. In offshore waters where there are minimal suspended sediments, the patchiness associated with chlorophyll variation is observed in the 443 channel (Fig. 20).

The Landsat image (Fig. 21) was collected two hours earlier than CZCS and is channel 2 (600-700 nm) enhanced for the water features. The Landsat image has increased resolution than what is illustrated in Figure 20 and is clearly superior to CZCS in recognition of coastal features. At full resolution of Landsat, additional water features are observed within the coastal region that are not observed at the resolution displayed in Figure 21. The spatial resolution is significant in evaluating satellite applications in coastal areas (Arnone, 1983b). Coastal features are even more numerous and more detectable with increasing resolution, beyond the 80 m resolution of Landsat. The boundaries of land/water and coastal water masses are determined better by Landsat than by CZCS. Coastal boundary recognition is limited by the spatial resolution of CZCS. Shadowing effects bordering the barrier islands are observed in magnified coastal areas of Figure 20. The large pixel resolution effectively averages the coastal water color fronts. Upon close examination, the turbid waters of northern Mississippi Sound (stations 6 and 41) are illustrated as lighter tones in Figure 21 and a dark upwelling signal at 670 nm. The atmospheric correction results in negative, or dark tones, in Figure 20. In these type coastal areas proper considerations must be applied to interpreting the effects of the atmospheric correction.

The spectral differences between CZCS and Landsat are also illustrated in Figures 20 and 21. Numerous offshore oceanic features are observed in the 443 channel of CZCS. Since this channel was designed to respond to chlorophyll variability, the patchiness of the offshore waters is clearly visible. These features are not observed with the Landsat sensor. The 520 and 550 nm channels of CZCS respond more closely to the green (band 1) and red (band 2) of Landsat. The variations of suspended sediment are observed with both the Landsat and CZCS sensors by comparison of these channels.

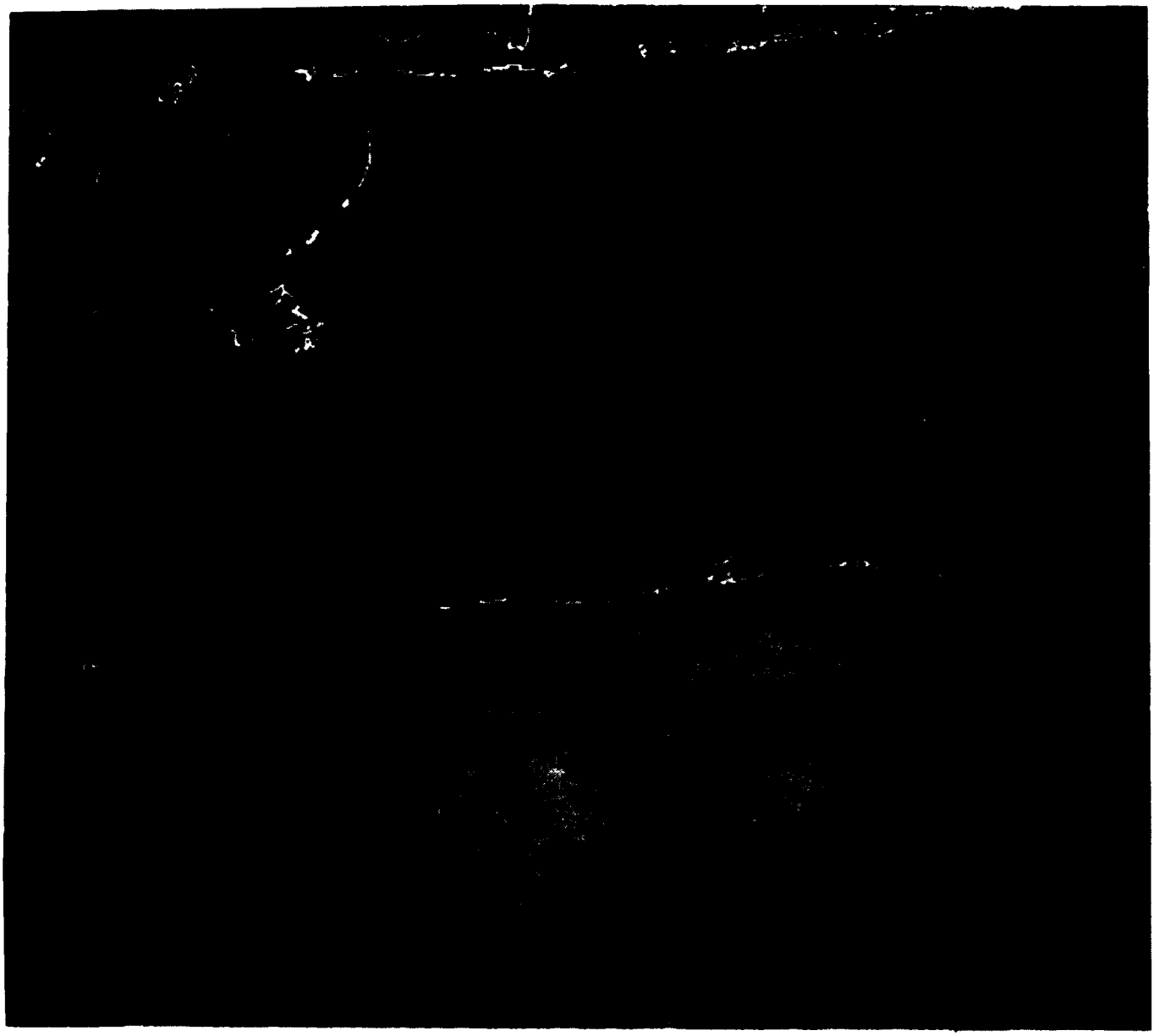

Figure 20. CZCS imagery atmospherically corrected, 14 September 1980, channels 443 and 520 nm

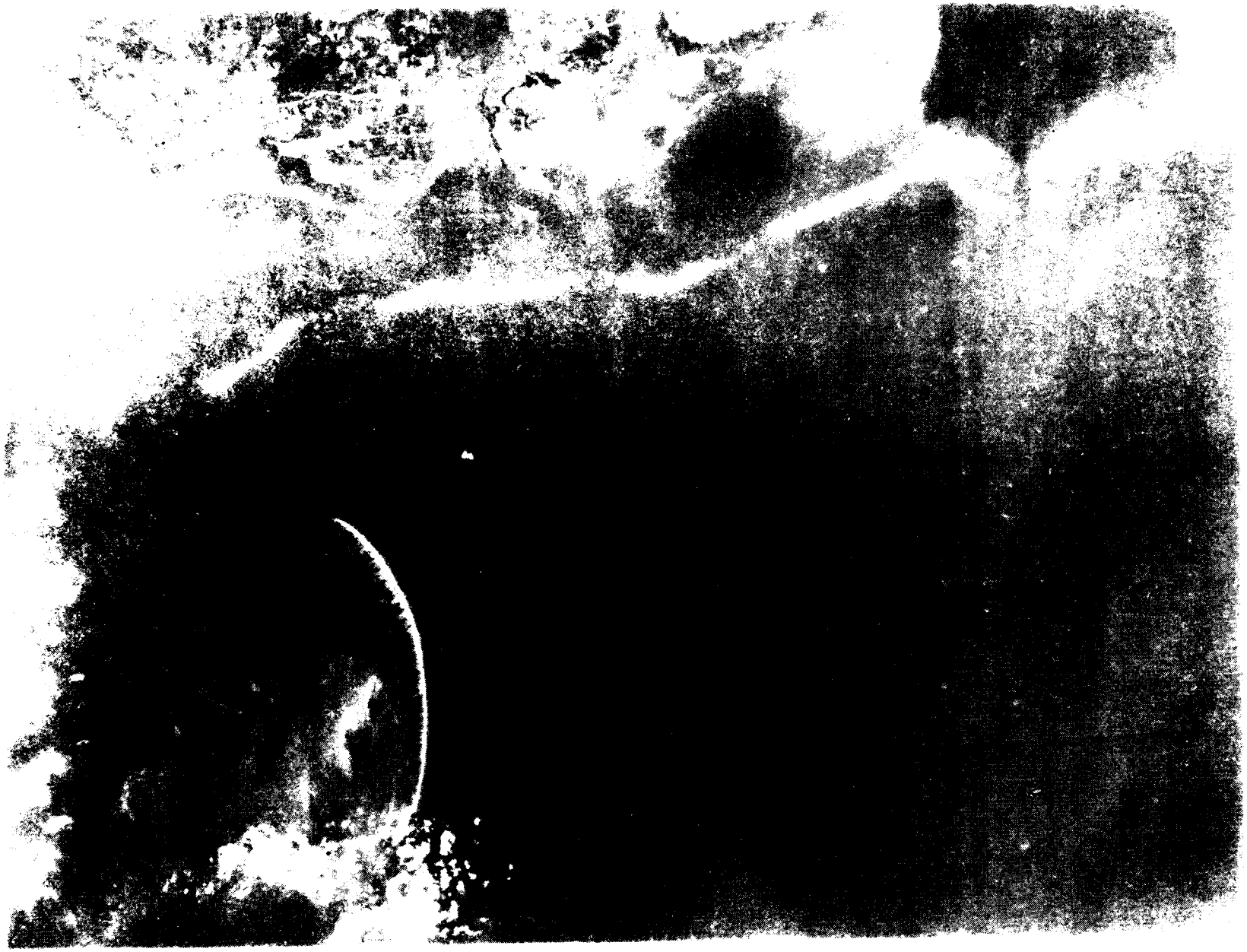

Figure 21. Landsat imagery, 14 September 1980, Band 5 (600-700 nm)

2. 15 September 1980

Landsat and CZCS imagery for September 15 are illustrated in Figures 22 and 23. Unfortunately, no ground truth was collected on this date for comparison. Figure 22 is band 5 of Landsat and covers only the western portion of the sound. Comparison of the 14-15 September Landsat images (Figs. 21, 22) indicated a high suspended sediment concentration in the northern sound, offshore of the Gulfport area. Only minor variations in the sediment patchiness are noticed between the two figures. It is difficult to observe any subtle variations of water color in these figures especially offshore of the barrier islands as a result of Landsat's low dynamic range sensors.

Figure 23 is a CZCS image from 15 September 1980. The upper part of this image is the 443 nm channel and the lower portion is the 520 nm channel. Both images have been atmospherically corrected using the 670 nm channel. Notice in this image a distinctive white band crossing the lower portion of the delta and extending toward the northeast. This represents a thick aerosol air mass much different from that observed on 14 September (Fig. 20) and has significantly different angstrom values for coastal and offshore ocean waters. For this image the coastal waters have been enhanced and the offshore waters are saturated. Similarities in the distribution of suspended sediments are observed in the CZCS (Figs. 20, 23). The sediment plumes extending through the channels between the barrier islands are clearly observed. Comparison of CZCS with Landsat imagery illustrates the applications that Landsat resolution has in showing coastal features. The detection of the more subtle water colors occurring in offshore waters are better observed in CZCS imagery.

3. 24 September 1980

The CZCS imagery for 24 September is contaminated by a large percentage of clouds. However, there appears to be certain areas of the image in which cloud free conditions and ground truth were collected. Data on 24 September was collected at Stations t4 through t40 which is the central part of the Mississippi Sound (see Fig. 1). The relationship between the raw counts and the suspended sediment concentrations is illustrated in Figure 24 for the 443 and 550 nm channels. From the linear fit of this relationship, the sediment type in this area appears to be uniform, not like that shown on 9 September. The 550 nm channel has a regression coefficient of 0.91. This is the best correlation compared with the two other bands and reinforces the ability of the 550 nm sensitivity to suspended sediments. By comparison of this figure with results of 9 September (Figs. 17-19), the overall count was higher on the 24 September. Note that the imagery has not been atmospherically corrected, and that these regressions can not be utilized in the universal sense. Results of the atmospherically corrected imagery for the 9 and 24 September comparison with ground truth showed similar nonuniversal results. This was attributed to the erroneous assumption of zero upwelling radiation in the 670 nm band, as was mentioned earlier.

The relationship between secchi depth and raw count values for 24 September is illustrated in Figure 25 for the 520 and 550 nm channels. A high linear correlation coefficient for the 550 nm channel (0.87) indicates a similar influence of suspended sediment concentration and this spectral channel observed in Figure 24. Increased count values indicate high suspended sediments and lower secchi depths. The

Figure 22. Landsat imagery, 15 September 1980, Band 5 (600-700 nm)

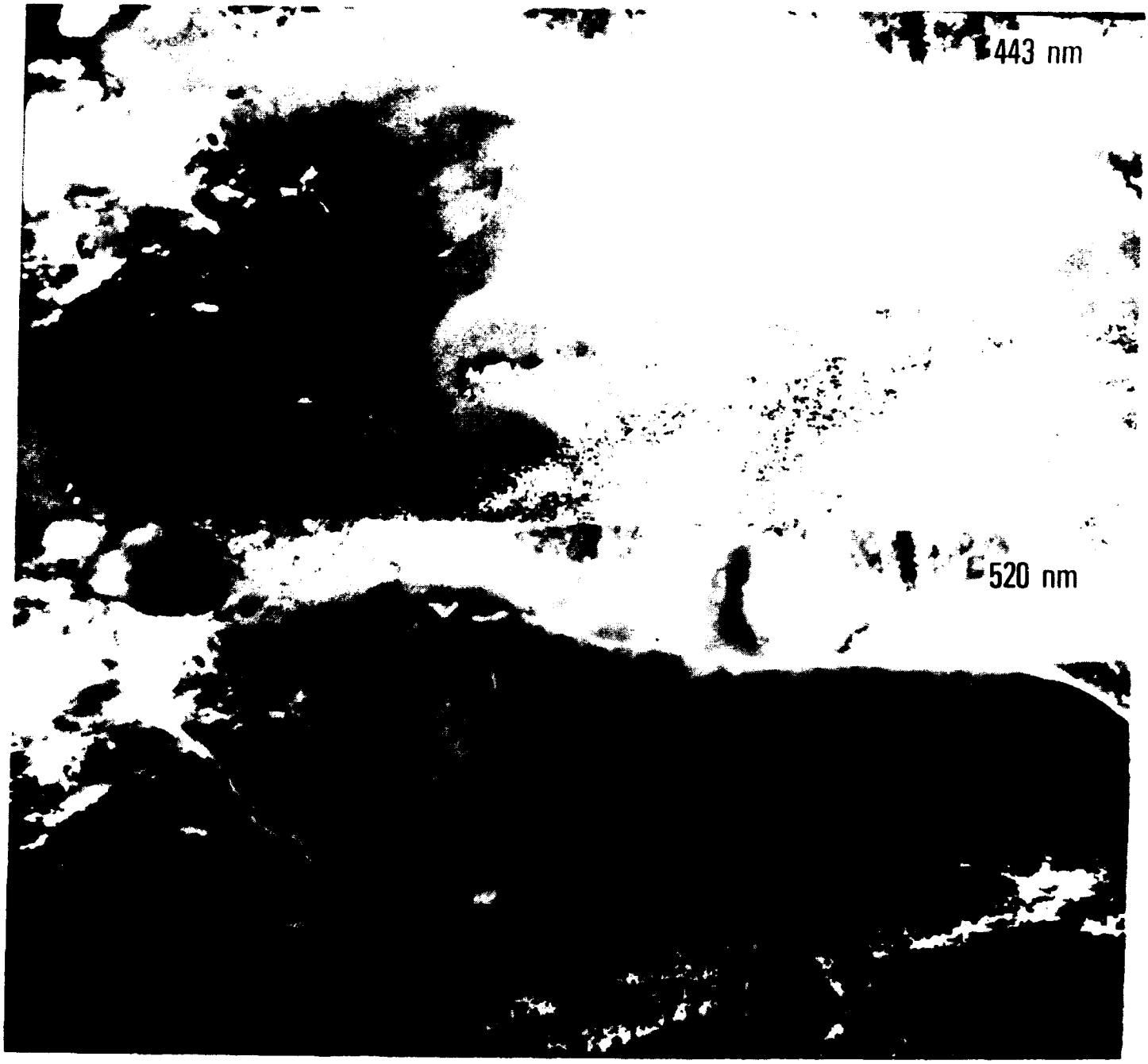

Figure 23. CZCS imagery atmospherically corrected, 15 September 1980, channels 443 and 520 nm

relatively high correlation coefficients for both these spectral channels indicate that the partical size, shape, and composition of the suspended sediments was uniform at the sample locations. (The w(k') illustrated in Figures 5 and 6 would be constant.)

The relationship of the raw count values of CZCS and the diffuse attenuation coefficients (k) is somewhat disturbing. One would expect a strong relationship between count values and "k" since "k" is inversely related to secchi depth. This should be further enforced by the two previous figures (Fig. 24, 25) which showed strong correlation. Figure 26 shows the correlation between the downwelling spectral

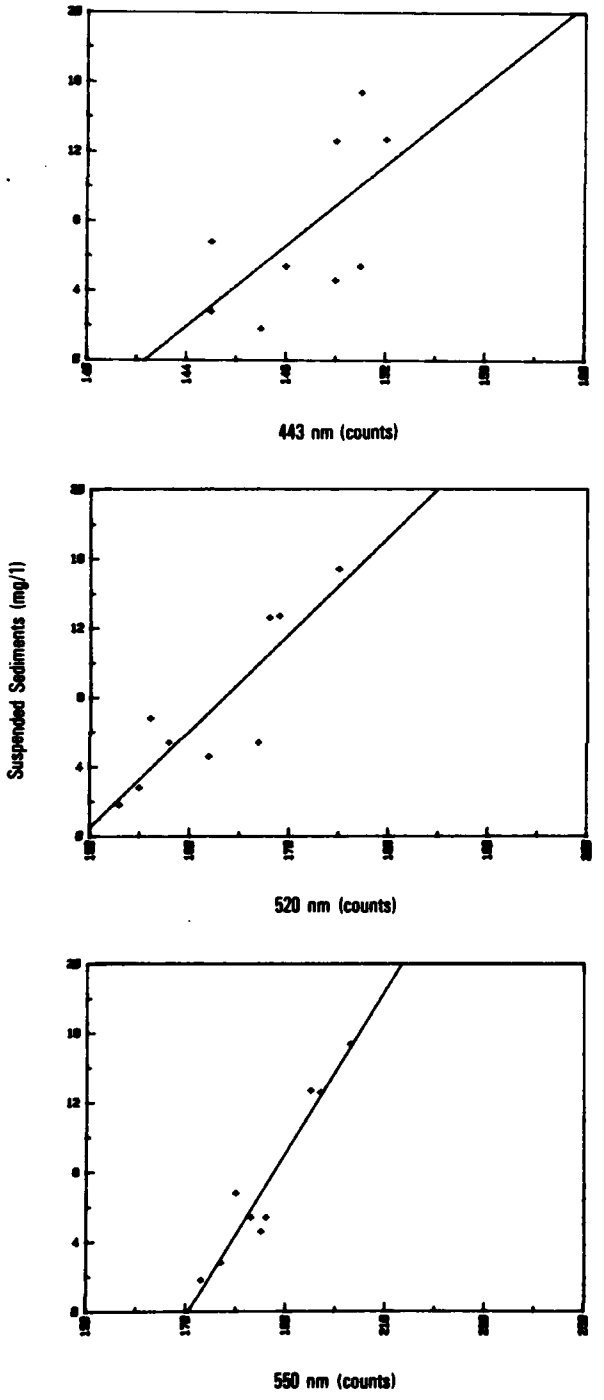

Figure 24. Correlation of CZCS count values, 24 September 1980, and total suspended sediments

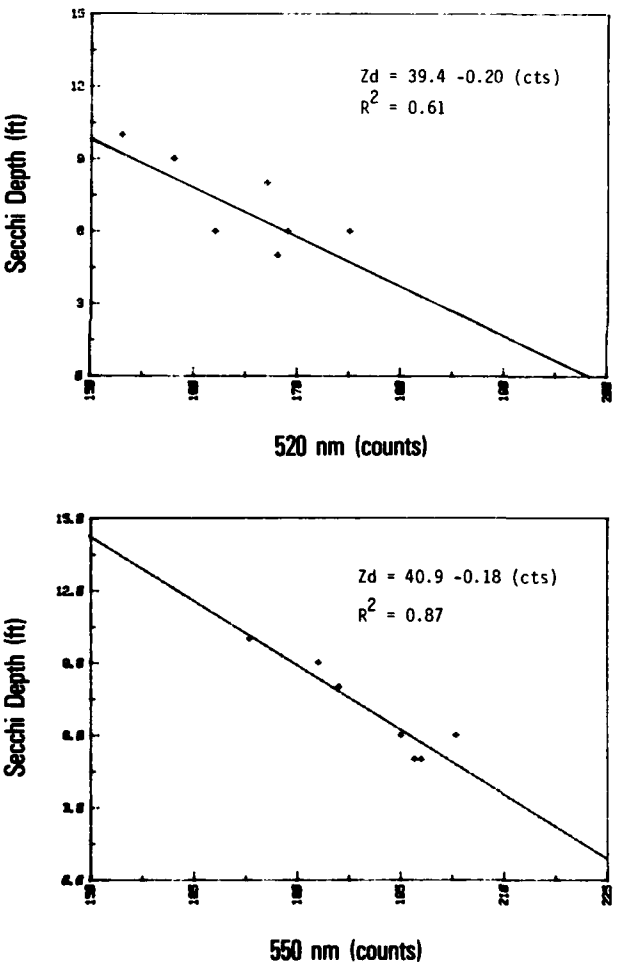

Figure 25. Correlation of CZCS count values, 24 September 1980, and secchi depth

diffuse attenuation coefficient and the CZCS count values at each wavelength. A strong linear correlation is observed at the 443 nm wavelength (R = 0.58).

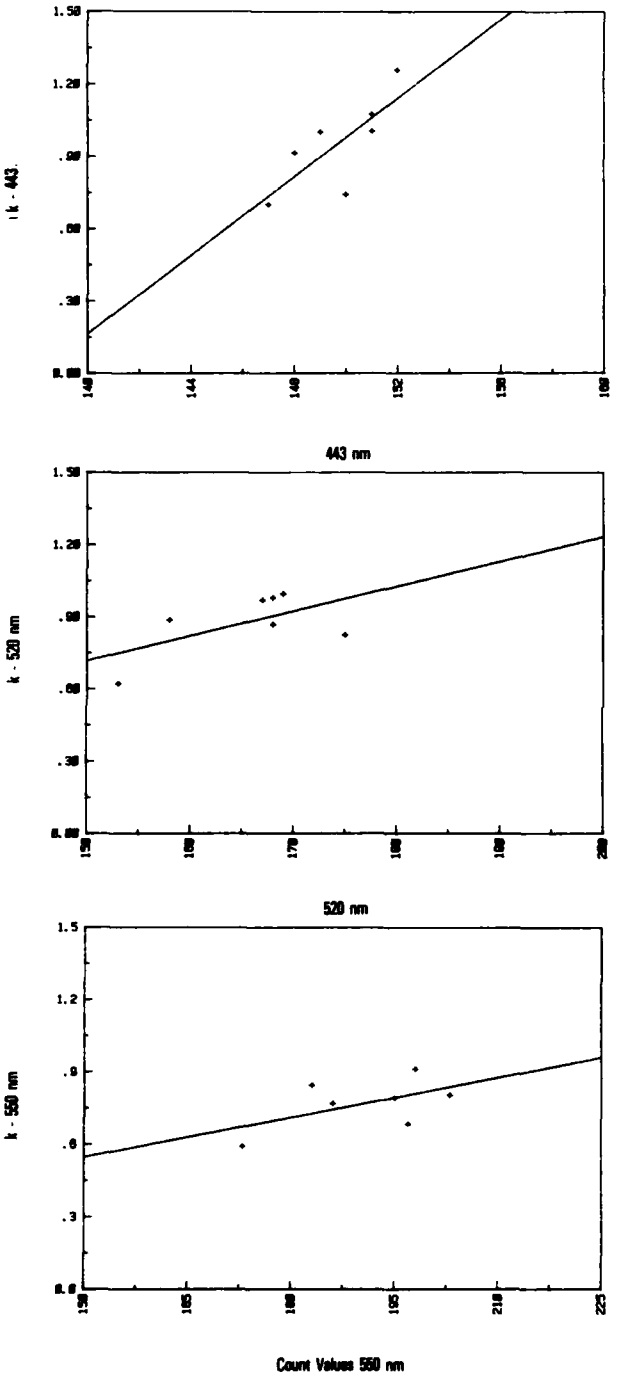

Figure 26. Correlation of CZCS count values, 24 September 1980, and "K_d"

The 520 nm channel shows a weaker correlation (R = 0.35) and finally the 550 nm channels show less of a correlation (R = 0.30).

The lower correlation in the 550 nm channel indicates that the downwelling diffuse attenuation coefficient (k_d) is not strongly correlated with the radiance as viewed by the satellite. The relationship of downwelling attenuation coefficients and backscattering radiation (as sensed by secchi depths and upwelling radiance) was discussed in the first section of the report. A similar spectral response of this channel was observed in that the relationship of upwelling to downwelling radiation had the weakest correlation in the 550 nm channel (Fig. 12, Table 5). A similar explanation can be applied to the noted correlation in Figure 26. A CZCS image for 24 September is illustrated in Figure 27. This image is a simple density slice of the 520 nm channel in which the linear regression shown in Figure 24 was applied to obtain a suspended sediment concentration of the sound. From this image, it is evident that the numerous clouds make the water areas difficult to classify.

VI. Conclusions

Results of the satellite data processing for the Mississippi Sound Experiment indicate complicated processes occurring both in the temporal and spacial domain. The sound's response to tides and local winds directly affects the circulation which in turn results in variations in the water types. The movements of the water masses result in turbulent mixing and diffusion, all of which change the characters of the upwelling radiance that are observed by satellite.

The suspended sediment concentration dominates the turbidity patterns and optical properties within the Mississippi Sound. The satellite received radiance is also dominated by suspended sediments. Unfortunately, the size,

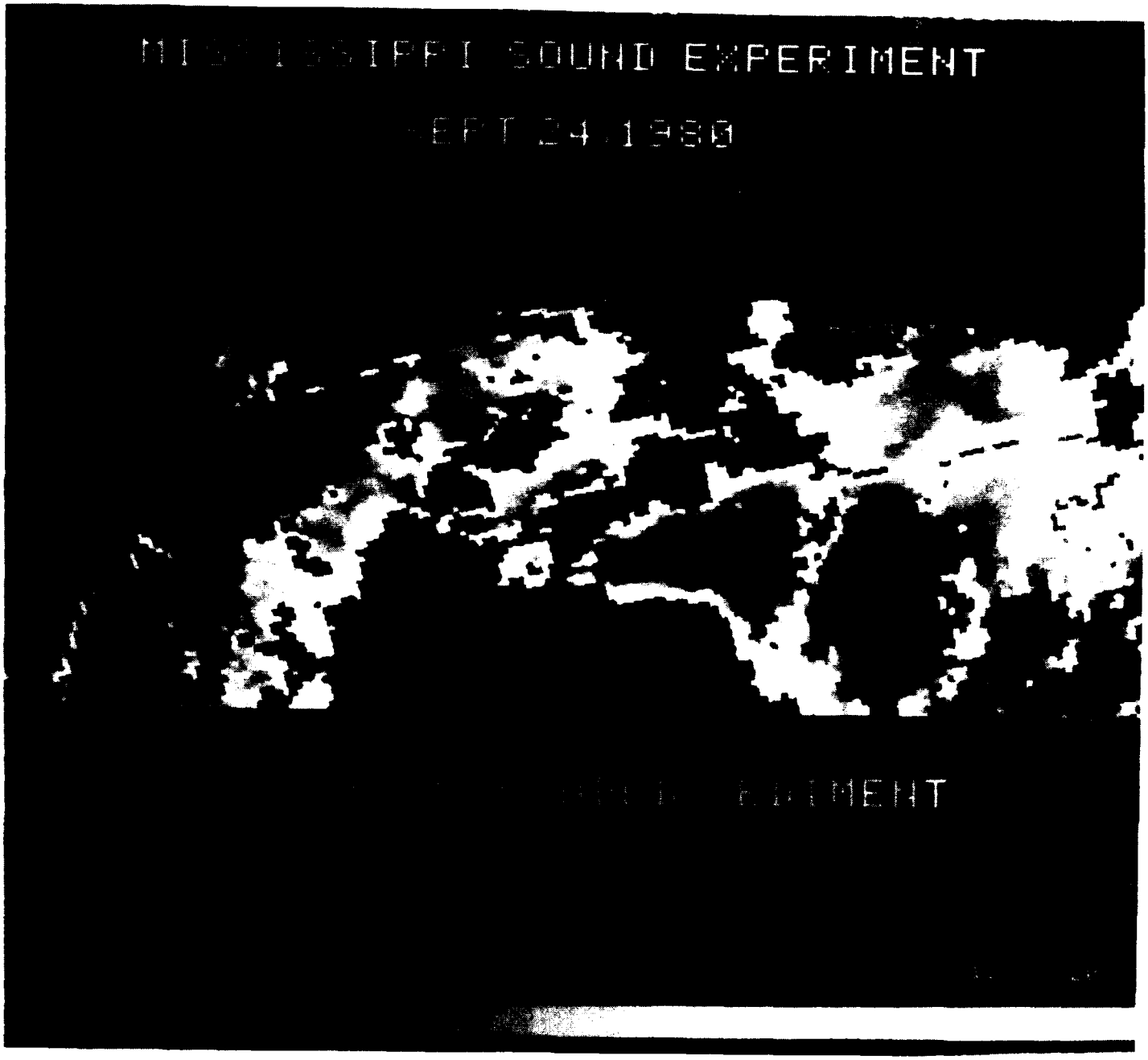

Figure 27. Suspended sediment concentration derived from CZCS, 24 September 1980, from channel 550 nm

shape, and composition, in addition to the concentration, interact to determine optical and upwelling radiance properties.

Specific optical properties within the sound were shown to be correlated. It is necessary to determine the applications of these regression relationships on other water types to establish the validity of these relationships and to extend the applicability to various water types.

The optical properties of Mississippi Sound waters are different and much more complicated than the offshore oceanic waters. The composition, temporal, and spacial variability of coastal waters have significant differences on the optical properties compared to either shelf or deep oceanic waters. The extension of coastal water types into the offshore regions is becoming more evidenced through analyses of satellite imagery. The response of coastal water types in changing the optical water character, both temporally and on radiance measurements from a satellite, will provide an improved understanding of the chemical and physical dynamics of the ocean.

The application of "universal" algorithms to determine the diffuse attenuation coefficient, chlorophyll concentration, and total suspended sediments, requires absolute spectral measurement of upwelling radiation from the water column. Satellite data must be accurately atmospherically corrected to obtain the upwelling radiation measurement. Current atmospheric correction techniques appear to be confined to deeper oceanic waters. Tests of universal algorithms in coastal waters resulted in nonability to adequately correct for the atmosphere. Problems with nonzero upwelling radiation in the reference channel and varying angstrom coefficients within the image were experienced. Additional corrections are required for coastal waters.

The utility of both CZCS and Landsat systems to detect coastal features and water properties is related to both the spacial resolution and spectral differences of coastal water properties. For the study area, the spacial variability of the coastal water properties significantly influenced the evaluation of CZCS and Landsat. If the upwelling radiation from the water column is significantly strong, as is the case in many coastal areas, then Landsat's high resolution is significant. As the upwelling radiation becomes reduced and the water color variability is more subtle, then the spectral resolution and increased dynamic range of the CZCS sensor appears more significant. From comparison of near-coincident Landsat and CZCS imagery as the water color becomes more subtle the water patterns appear to increase in size, such that increased resolution of CZCS can be used to detect the variability.

VII. References

Ahern, F. J. and J. Murphy (1978). Radiometric Calibration and Correction of Landsat, 1, 2, and 3 MSS Data. Research Report 78-4, Canada Centre for Remote Sensing, Department of Energy, Mines, and Resources, Ottawa, Canada.

Aranuvachapun, S. and P. LeBlond (1981). Turbidity of the Coastal Water Determined from Landsat Remote Sensing of Environment. vol. 84, pp. 113-132.

Aranuvachapun, S. and R. J. Perry (1981). Spectral Variations of Coastal Waters Irradiance as a Measure of Phytoplankton Pigements. Int. J. Remote Sensing, vol. 2, pp. 299-312.

Arnone, R. A. (1983). Spacial Variations of Coastal Features Measured from Landsat. Naval Ocean Research and Development Activity NSTL, Miss. (in preparation).

Austin, R. W. (1980). Gulf of Mexico, Ocean-Color Surface-Truth Measurements.

Boundary Layer Meteorology, vol. 18, pp. 269-285.

Austin, R. W. and T. J. Petzold (1980). The Determination of the Diffuse Attenuation Coefficient of Sea Water Using the Coastal Zone Color Scanner. COSPAR/SCOR/IUCRM Symposium, Oceanography from Space, 26-30 May, Venice, Italy.

Clark, D. R., E. T. Baker, and A. E. Strong (1980). Upwelled Spectral Radiance Distribution in Relation to Particulate Matter in Sea Water. Boundary Layer Meteorology, vol. 18, pp. 287-298.

Gordon, H. R. (1978). Removal of Atmospheric Effects from Satellite Imagery of the Oceans. Applied Optics, vol. 17, No. 10.

Gordon, H. R. and D. K. Clark (1980). Atmospheric Effects in the Remote Sensing of Phytoplankton Pigments. Boundary Layer Meteorology, vol. 18, pp. 299-313.

Gordon, H. R. and D. K. Clark (1981). Clear Water Radiances for Atmospheric Correction of Coastal Zone Color Scanner Imagery. Applied Optics, vol. 20, No. 24.

Gordon, H. R. and A. W. Wouters (1978). Some Relationships Between Secchi Depth and Inherent Optical Properties of Natural Waters. Applied Optics, vol. 17, No. 21.

Holmes, R. W. (1970). The Secchi Disk in Turbid Coastal Waters. Limnal. Oceanography, vol. 15, pp. 688.

Holyer, R. (1978). Toward Universal Multispectral Suspended Sediment Algorithms. Remote Sensing of Environment, pp. 323-338.

Hovis, W. A., D. K. Clark, F. Anderson, R. W. Austin, W. A. Wilson, E. I. Butler, D. Ball, H. R. Gordon, J. L. Mueller, S. F. El-Sayed, B. Sturm, R. C. Wrigley, and C. S. Yentsch (1980). Nimbus-7 Coastal Zone Color Scanner: System Description and Initial Imagery. Science, vol. 210 (4465). pp. 60-63.

Isphording, W. C. (1981). Mississippi Sound Hydrodynamic Data. Array Corps. of Engineers, Mobile District. Contract No. DACWO 1-80-M-C169.

Manheim, F. T, Meade, R. H., and Bond, G. C. (1970). Suspended Matter in Surface Waters of the Atlantic Continental Margin from Cape Code to the Florida Keys. Science, vol. 167, pp. 371.

Munday, J. C. and T. T. Alfoldi (1979). Landsat Test of Diffuse Reflectance Models for Aquatic Suspended Solids Measurements. Remote Sensing of Environment, vol. 8, pp. 169-183.

Pool, H. H. and W. R. Atkins (1929). Photo-Electric Measurements of Submarine Illumination Throughout the Year. J. Mar. Bio. Assoc. U.K., vol. 16, pp. 297.

Raytheon Inc. (1981). Mississippi Sound Data Collection Program. Final Report, Vol. I, Army Corp. of Engineers, Mobile District. Contract No. DACWO 1-80-C-0104.

Sheng, Y. P. (1983). Mathematical Modeling of Three-Dimensional Coastal Currents and Sediment Dispersion. Vol. 1, Model Development and Application, Aeronautical Research Associates of Princeton, Inc. ARAP Report #486.

Sheng, Y. P. and Butler, H. L. (1982). Modeling Coastal Currents and Sediment Transport; Proceedings of the 18th Conference on Coastal Engineering, ASCE Capetown, Nov. 14-18.

Distribution List

Department of the Navy
Asst Deputy Chief of Navy Materials
for Laboratory Management
Rm 1062 Crystal Plaza Bldg 5
Washington DC 20360

Department of the Navy
Asst Secretary of the Navy
(Research Engineering & System)
Washington DC 20350

Project Manager
ASW Systems Project (PM-4)
Department of the Navy
Washington DC 20360

Department of the Navy
Chief of Naval Material
Washington DC 20360

Department of the Navy
Chief of Naval Operations
ATTN: OP 951
Washington DC 20350

Department of the Navy
Chief of Naval Operations
ATTN: OP 952
Washington DC 20350

Department of the Navy
Chief of Naval Operations
ATTN: OP 987
Washington DC 20350

Director
Chief of Naval Research
ONR Code 420
Ocean Science & Technology Det
NSTL, MS 39529

Director
Defense Technical Info Cen
Cameron Station
Alexandria VA 22314

Commander
DW Taylor Naval Ship R&D Cen
Bethesda MD 20084

Commanding Officer
Fleet Numerical Ocean Cen
Monterey CA 93940

Director
Korean Ocean R&D Inst
ATTN: K. S. Song, Librarian
P. O. Box 17 Yang Jae
Seoul South Korea

Commander
Naval Air Development Center
Warminster PA 18974

Commander
Naval Air Systems Command
Headquarters
Washington DC 20361

Commanding Officer
Naval Coastal Systems Center
Panama City FL 32407

Commander
Naval Electronic Sys Com
Headquarters
Washington DC 20360

Commanding Officer
Naval Environmental Prediction
Research Facility
Monterey CA 93940

Commander
Naval Facilities Eng Command
Headquarters
200 Stovall St.
Alexandria VA 22332

Commanding Officer
Naval Ocean R & D Activity
ATTN: Codes 110/111
Code 125
Code 200
Code 300
Code 115
Code 500
NSTL MS 39529

Director
Liaison Office
Naval Ocean R & D Activity
800 N. Quincy Street
502 Ballston Tower #1
Arlington VA 22217

Commander
Naval Ocean Systems Center
San Diego CA 92152

Commanding Officer
Naval Oceanographic Office
NSTL MS 39522

Commander
Naval Oceanography Command
NSTL MS 39522

Superintendent
Naval Postgraduate School
Monterey CA 93940

Commanding Officer
Naval Research Laboratory
Washington DC 20375

Commander
Naval Sea System Command
Headquarters
Washington DC 20362

Commander
Naval Surface Weapons Center
Dahlgren VA 22448

Commanding Officer
Naval Underwater Systems Center
ATTN: New London Lab
Newport RI 02840

Director
New Zealand Oceano Inst
ATTN: Library
P. O. Box 12-346
WELLINGTON N., NEW ZEALAND

Director
Office of Naval Research
Ocean Science & Technology Div
NSTL MS 39529

Department of the Navy
Office of Naval Research
ATTN: Code 102
800 N. Quincy St.
Arlington VA 22217

Commanding Officer
ONR Branch Office
536 S Clark Street
Chicago IL 60605

Commanding Officer
ONR Branch Office LONDON
Box 39
FPO New York 09510

Commanding Officer
ONR Western Regional Ofs
1030 E. Green Street
Pasadena CA 91106

President
Texas A&M
ATTN: Dept of Ocean Working Collection
College Station TX 77843

Director
University of California
Scripps Institute of Oceanography
P. O. Box 6049
San Diego Ca 92106

Director
Woods Hole Oceanographic Inst
Woods Hole MA 02543

UNCLASSIFIED

SECURITY CLASSIFICATION OF THIS PAGE *(When Data Entered)*

REPORT DOCUMENTATION PAGE		READ INSTRUCTIONS BEFORE COMPLETING FORM
1. REPORT NUMBER NORDA Report 63	2. GOVT ACCESSION NO. AD-A139825	3. RECIPIENT'S CATALOG NUMBER
4. TITLE *(and Subtitle)* Water Optics of the Mississippi Sound		5. TYPE OF REPORT & PERIOD COVERED Final
		6. PERFORMING ORG. REPORT NUMBER
7. AUTHOR(s) Robert A. Arnone		8. CONTRACT OR GRANT NUMBER(s)
9. PERFORMING ORGANIZATION NAME AND ADDRESS Naval Ocean Research and Development Activity NSTL, Mississippi 39529		10. PROGRAM ELEMENT, PROJECT, TASK AREA & WORK UNIT NUMBERS PE62759N
11. CONTROLLING OFFICE NAME AND ADDRESS Naval Ocean Research and Development Activity NSTL, Mississippi 39529		12. REPORT DATE December 1983
		13. NUMBER OF PAGES 39
14. MONITORING AGENCY NAME & ADDRESS*(if different from Controlling Office)*		15. SECURITY CLASS. *(of this report)* Unclassified
		15a. DECLASSIFICATION/DOWNGRADING SCHEDULE

16. DISTRIBUTION STATEMENT *(of this Report)*

Approved for Public Release
Distribution Unlimited

17. DISTRIBUTION STATEMENT *(of the abstract entered in Block 20, if different from Report)*

18. SUPPLEMENTARY NOTES

19. KEY WORDS *(Continue on reverse side if necessary and identify by block number)*

optics
satellite
oceanography
coastal processes
CZCS

20. ABSTRACT *(Continue on reverse side if necessary and identify by block number)*

From analyses of optical and suspended sediment properties in the Mississippi Sound, inherent relationships for exceptional turbid coastal waters are established. The optical parameters of secchi depth, Nepholometric Turbidity Units (NTU) and spectral upwelling and downwelling diffuse attenuation coefficients are correlated with themselves and size distribution of suspended sediments. From these relationships, estimates of other scattering and absorption water optical properties are established.

(continued)

DD FORM 1 JAN 73 1473 EDITION OF 1 NOV 65 IS OBSOLETE
S/N 0102-LF-014-6601

UNCLASSIFIED

SECURITY CLASSIFICATION OF THIS PAGE *(When Data Entered)*

(continued from Block 20)

Coastal Zone Color Scanner (CZCS) and Landsat satellite data coincident with the experimental data were analyzed to access the spatial, temporal and quantitative optical properties with the sound and surrounding shelf waters. Problems with atmospheric correction techniques in turbid coastal waters precluded obtaining quantitative optic measurements. Relationships between the spectral satellite radiance values and optical properties are established.